Modeling Coupled THM Processes and Reactive Diffusive Transport in Engineered Barrier Systems (EBS)

Jonny Rutqvist, Carl Steefel, Juan Galindez, Jens Birkholzer, and Hui-Hai Liu

Lawrence Berkeley National Laboratory (LBNL)

Table of Contents

1. Introduction 5
2. THM Modeling of EBS Including Buffer-Rock Interaction 6
2.1 Base-case simulation results ... 6
2.2 Thermal management study and peak temperature ... 11
2.3 Resaturation time and buffer swelling ... 14
2.4 Rock failure for layered rock ... 15
2.5 Model development and code implementation of double-structure constitutive model for bentonite ... 18
3. Reactive Diffusion in Bentonite 19
3.1 Experimental investigation of diffusion through compacted bentonite ... 20
3.2 Single type pore model ... 23
3.3 Double type pore model ... 29
3.4 Analytical solution ... 34
4. Knowledge Gaps and Future Work 39
4.1 Knowledge gaps ... 39
4.2 Future work in FY11 and FY12 ... 42
5. Recommended Areas of International Collaboration 43
5.1 Opportunities and considerations ... 43
5.2 DECOVALEX Project ... 46
5.3 Mont Terri Project ... 50
5.4 Colloid Formation and Migration (CFM) Project ... 53
5.5 Other active collaboration opportunities ... 55
5.6 Recommendations and path forward ... 58
6. Summary 59
7. References 61

List of Figures

Figure 2.1. Model domain for an assumed bentonite back-filled horizontal emplacement drift at 500 m depth in clay host rock. ... 7

Figure 2.2. Simulated evolution of THM processes in buffer: (a) temperature, (b) liquid saturation, (c) fluid pressure, and (d) total radial stress (σx). See Figure 2.1 for locations of V1, V2, V3, and V6. ... 10

Figure 2.3. Calculated evolution of stresses: (a) stress evolution a point V3 located at the tunnel wall, and (b) stress evolution at point V6 located 10 m away from the tunnel. See Figure 2.1 for locations of V3 and V6. ... 11

Figure 2.4. Calculated principal stress path at point V3 located at the tunnel wall. ... 11

Figure 2.5. Calculated evolution of (a) liquid saturation and (b) temperature in the case of a buffer consisting of granular bentonite with 1% initial saturation. ... 13

Figure 2.6. Calculated temperature evolution for the extreme case densely spaced waste canisters (reduced canister and tunnel spacing) and a buffer consisting of granular bentonite with 1% initial saturation, as well as a low thermal conductivity of the rock. . 14

Figure 2.7. Time to 99% saturation for different values of rock-mass permeability. 15

Figure 2.8. (a) Volumetric strain and (b) shear strain in the rock at 100,000 years for the case of anisotropic strength properties (the orientation of the bedding planes are indicated). 17

Figure 2.9. Calculated stress path for the case of anisotropic strength properties of the host rock. 18

Figure 3.1. Schematic view of the experimental setup used in the through-diffusion experiment (from Van Loon et al., 2007). 20

Figure 3.2. Logarithmic representation of the dependence of ^{c}D *and Rd for* $^{22}Na^{+}$ *(Plot A) and* $^{85}Sr^{2+}$ *(Plot B) on the cation concentration in the external water phase [A]. The data are mean values of results from through-diffusion experiments and profile analysis; 5 mm and 10 mm clay thickness (from Glaus et al., 2007).* 23

Figure 3.3. Tracer concentration profile at steady state for chloride through-diffusion. For typical experimental setups, the transport capacity of the filters is large enough to supply the clay with anions, and the full concentration drop occurs within the clay. Thus, filters do not need to be considered for evaluation of clay chloride diffusivity (from Birgersson and Karnland, 2009). 24

Figure 3.4. Spatial distribution of concentration of chloride as modeled by Birgersson and Karnland (2009). 25

Figure 3.5. Fit of experimental data reported by Van Loon et al. (2007) obtained by the single type pore model: (a) 1300 kg/m^{3}*, (b) 1600 kg/m*^{3}*, (c) 1900 kg/m*^{3} 29

Figure 3.6. Spatial distribution of concentration of chloride as modeled in CrunchFlow. 32

Figure 3.7. Fit of experimental data reported by Van Loon at al. (2007) obtained by the single type pore model: (a) 1300 kg/m^{3}*, (b) 1600 kg/m*^{3}*, (c) 1900 kg/m*^{3} 34

Figure 3.8. Normalized profiles of concentration of chloride obtained with varying ionic strength for a range of dry density values (a) 1300 kg/m^{3}*; (b) 1600 kg/m*^{3}*; (c) 1900 kg/m*^{3}*.* 37

Figure 3.9. Fit of experimental data reported by Van Loon at al. (2007) obtained by the analytical solution of the simplified form of the Poisson-Boltzmann equation for the case of a binary solution between two parallel plates: (a) 1300 kg/m^{3}*; (b) 1600 kg/m*^{3}*; (c) 1900 kg/m*^{3}*.* 39

Figure 5.1. Schematic setup of HE-E heater test at Mont Terri and photo of micro-tunnel (from Garitte et al, 2011) 48

Figure 5.2. Schematic setup of mini-tunnel with seal core and instrumentation (left); view from gallery after core emplacement (right) (from Barnichon, 2011) 49

Figure 5.3. Planned experiments and schedule (from Barnichon, 2011)..... 49

Figure 5.4. Geological cross-section of the Tournemire site, South France (from Rejeb and Cabrera, 2006) (from Barnichon, 2011) 50

Figure 5.5. Summary schematic of the Mont Terri URL with side galleries and drifts for testing (based on Garitte, 2010) 52

Figure 5.6. Plan (top) and side view (bottom) of experiment setup and observation borehole layout (from Garitte, 2010)..... 53

Figure 5.7. Schematic setup of bentonite plug and colloid transport experiment (from http://www.grimsel.com/gts-phase-vi/cfm-section/cfm-concept)..... 55

Figure 5.8. Layout of the PRACLAY In-Situ Experiment which is constituted of the the Seal Test, and the actual Heater Test (from Van Marcke and Bastiaens, 2010)..... 56

Figure 5.9. Schematic picture of repository seal design for GAST experiment (from Vomvoris, 2011)..... 57

Figure 5.10. GASIT experiment at Äspö (from Cuss, 2010)..... 57

List of Tables

Table 2-1. Thermal and hydraulic properties of the bentonite buffer. 7

Table 2-2. BBM material parameter for the bentonite buffer..... 8

Table 2-3. THM rock properties for the clay stone host rock...... 9

Table 2-4. Material properties of the ubiquitous joint model...... 16

Table 3-1. Effective diffusion coefficients reported by Van Loon et al. (2007) as a function of dry density of clay and sodium chloride concentration in the pore water. 22

Table 3-2. Values of electrical potential at the shear plane and of semispacing between clay layers as a function of dry density obtained by fitting procedures of experimental data reported by Van Loon et al. (2007)...... 37

Table 5-1. Summary of UNF and HLW Management Programs in Other Countries 44

1. Introduction

Geological repositories for disposal of high-level nuclear wastes generally rely on a multi-barrier system to isolate radioactive wastes from the biosphere. The multi-barrier system typically consists of the natural barrier system (NBS), which includes the repository host rock and its surrounding subsurface environment, and the engineered barrier system (EBS). The EBS represents the man-made, engineered materials placed within a repository, including the waste form, waste canisters, buffer materials, backfill, and seals (OECD, 2003). The EBS plays a significant role in the containment and long-term retardation of radionuclide release.

During the lifespan of a geologic repository, the performance of the EBS is affected by complex thermal, hydrogeological, mechanical, chemical and biological processes, such as heat release due to radionuclide decay, multiphase flow (including gas release due to canister corrosion), swelling of buffer materials, radionuclide diffusive transport, waste dissolution and chemical reactions. All these processes are related to each other. An in-depth understanding of these coupled processes is critical for the performance assessment (PA) for an EBS and the entire repository. Within the EBS work package of the Used Fuel Disposition (UFD) Campaign, LBNL's research is currently focused on two relevant issues, namely the (1) thermal-hydraulic-mechanical-chemical (THMC) processes in buffer materials (bentonite), and the (2) diffusive transport in the EBS associated with clay host rock, with the long-term goal of developing a full understanding of (and verified modeling capabilities to simulate) the impact of coupled processes on radionuclide transport in different components of EBS, as well as the interaction between the near-field host rock (e.g., clay/shale) and EBS components—and how they affect radionuclide release.

LBNL's focus areas address key Features, Events and Processes (FEPs), which have been ranked in importance from medium to high as listed in Tables 7 and 8 of the *Used Fuel Disposition Campaign Disposal Research and Development Roadmap* (FCR&D-USED-2011-000065 REV0) (Nutt, 2011). Specifically, they address FEP 2.2.01, Excavation Disturbed Zone (EDZ), for shale by investigating the effects of coupled processes on interactions between shale (clay) disposal formations and the EBS; FEPs 2.1.04.01, Buffer/Backfill; FEPs 2.1.07.02, 03, 04, 09, Mechanical Processes; FEPs 2.1.08.03, 07, 08, Hydrologic Processes; and FEP 2.1.11.04, Thermal Processes, by studying coupled processes in the EBS; and FEPs 2.1.09.52, 53, 54, Chemical Processes—Transport by investigating reactive-diffusive radionuclide transport in bentonite.

This report documents the progress that LBNL has made in its two R&D focus areas. Section 2 presents the modeling results of geomechanical processes within bentonite and the interaction between EBS and a clay disposal formation in the near field. Section 3 documents the development of reactive-diffusive transport modeling approaches through bentonite in the EBS. Section 4 discusses identified knowledge gaps and technical issues, as well as near-term R&D plans. Section 5 follows with a description of opportunities for international collaborations. Work activities in the remaining months of FY11 and

integration between EBS and other UFD work packages are also discussed in the relevant sections.

2. THM Modeling of EBS Including Buffer-Rock Interaction

In FY10, LBNL incorporated the Barcelona Basic Model (BBM) into the TOUGH-FLAC simulator. The BBM is the most advanced and accepted constitutive model used for modeling of bentonite-buffer behavior in the various European and Japanese nuclear waste programs. In FY11, we have focused so far on using this new capability to model THM processes within a bentonite-backfilled emplacement tunnel and its interactions with the natural system (clay formations) and simulate the sensitivities of a number of processes and interactions to a variety of parameters. First, we present results for a base-case scenario that we developed during FY10 (Section 2.1 below) and then present results for a variety of parameter ranges from modeling conducted in FY11.

2.1 Base-case simulation results

In the base-case simulation scenario, we used clay host-rock properties derived from the Opalinus clay stone at Mont Terri, Switzerland (Gens et al., 2007). The EBS design featured waste emplacement in horizontal tunnels back-filled with bentonite-based swelling clays as a protective buffer (Figure 2.1). We adopted the heat load developed for the Generic Disposal System Environment (GDSE) within the UFD for Pressurized Water Reactor (PWR) used nuclear fuel. We adjusted tunnel and canister spacing to limit the maximum temperature to less than 100°C.

The basic material properties used for the base-case simulation scenario are presented in Tables 2-1 to 2-3. The bentonite properties, including the thermal and hydraulic properties (Table 2-1) and Barcelona Basic Model (BBM) properties (Table 2-2), were derived from laboratory experiments and *in situ* tests of FEBEX bentonite, whereas the rock properties correspond to that on Opalinus Clay (Table 2-3). The initial saturation of the bentonite buffer was set to 65%.

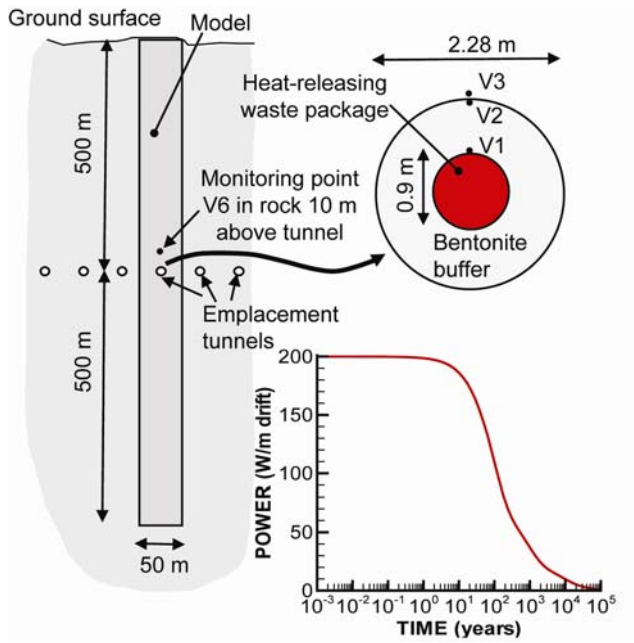

Figure 2.1. Model domain for an assumed bentonite back-filled horizontal emplacement drift at 500 m depth in clay host rock.

Table 2-1. Thermal and hydraulic properties of the bentonite buffer.

Parameter	Value/Function
Initial dry density, ρ_d [kg/m^3]	$1.6 \cdot 10^3$
Initial porosity, ϕ [-]	0.41
Saturated permeability, k [m^2]	$2.0 \cdot 10^{-21}$
Relative permeability, k_r [-]	$k_{rl} = S_l^3$
Van Genuchten's (1980) parameter, P_{VG} [MPa]	30
Van Genuchten's (1980) parameter, λ_{VG} [-]	0.32
Thermal expansion, β [1/°C]	$1.5 \cdot 10^{-4}$
Dry specific heat, C_s [J/kg·°C]	$c_s = 1.38T + 732.5$
Thermal conductivity, λ_m [W/m·°C]	$\lambda_m = 1.28 - \frac{0.71}{1 + e^{(S_l - 0.65)/0.1}}$
Effective vapor diffusion coefficient, D_v [m^2/s]	$D_v = 2.16e-5 \times \tau \times \phi \times S_g \left(\frac{T_{abs}}{273.8}\right)^{1.8}$
Tortuousity factor, τ [-]	0.8

Table 2-2. BBM material parameter for the bentonite buffer

Parameter	Value
Compressibility parameter for stress-induced elastic strain, κ_{PS0} [-]	0.05
Compressibility parameter for suction-induced elastic strain, κ_{SP0} [-]	0.25
Shear modulus, G [MPa]	NA
Poisson's ratio, ν [-]	0.4
Parameter for suction induced elastic strain, α_{SS} [-]	0
Parameter for stress-induced strain α_{PS} [MPa^{-1}]	-0.003
Parameter for stress-induced strain, α_{SP} [-]	-0.161
Reference stress state for relating elastic compressibility to suction, P_{ref} [MPa]	0.5
Parameters that relate elastic volumetric strain and temperature changes, α_0 [°C^{-1}]	1.5e-4
Compressibility parameter in virgin soil states at zero suction, λ_{PS0} [-]	0.15
Parameter defining soil stiffness associated with loading collapse yield, r_λ [-]	0.925
Parameter for the increase of soil stiffness with suction, β_λ [MPa^{-1}]	0.1
Parameter that relates cohesion to temperature, ρ_s [°C^{-1}]	0
Parameter describing the increase of cohesion with suction, k_s [-]	0.1
Tensile strength at saturated conditions, P_{S0} [MPa]	0
A reference stress state for compressibility relation in virgin states, P^C [MPa]	0.5
Slope of the critical state line, M [-]	1
Nonassociativity parameter in the plasticity flow rule, α_a [-]	0.53
Specific volume at reference stress states P^C in virgin states, v^c [-]	1.937
Net mean yield stress for saturated conditions at reference temperature, P^*_{0T} [MPa]	12.0

Table 2-3. THM rock properties for the clay stone host rock.

Parameter	**Value**
Bulk Density, [kg/m^3]	2400
Matrix Porosity [-]	0.15
Young's Modulus, [GPa]	5
Poisson's ratio, [-]	0.3
Specific heat, [J/kg·°C]	900
Thermal conductivity, [W/m·°C]	2.2
Thermal expansion coefficient, [°C^{-1}]	1.0×10^{-5}
Permeability, [m^2]	5.0×10^{-20}
Biot's effective stress parameter	1.0
Van Genuchten water retension parameter, *m*	0.41
Van Genuchten water retension parameter, P_0 [MPa]	48

We used the TOUGH-FLAC simulator and a new implementation of the Barcelona Basic Model (BBM) to model the coupled THM behavior of the bentonite. The simulations were conducted in the following sequence: (1) pre-excavation, (2) excavation, (3) waste and buffer emplacement, (4) post-closure coupled processes modeling. The results (Figure 2.2) show strong THM-driven interactions between the bentonite buffer and the low permeability host rock. The resaturation of the buffer is delayed as a result of the low rock permeability, and the fluid pressure in the host rock is strongly coupled with the temperature changes, resulting in a significant increase in pore pressure. This fluid pressure in excess of hydrostatic leads to an excess pressure gradient from the repository that lasts for up to 3,000 years.

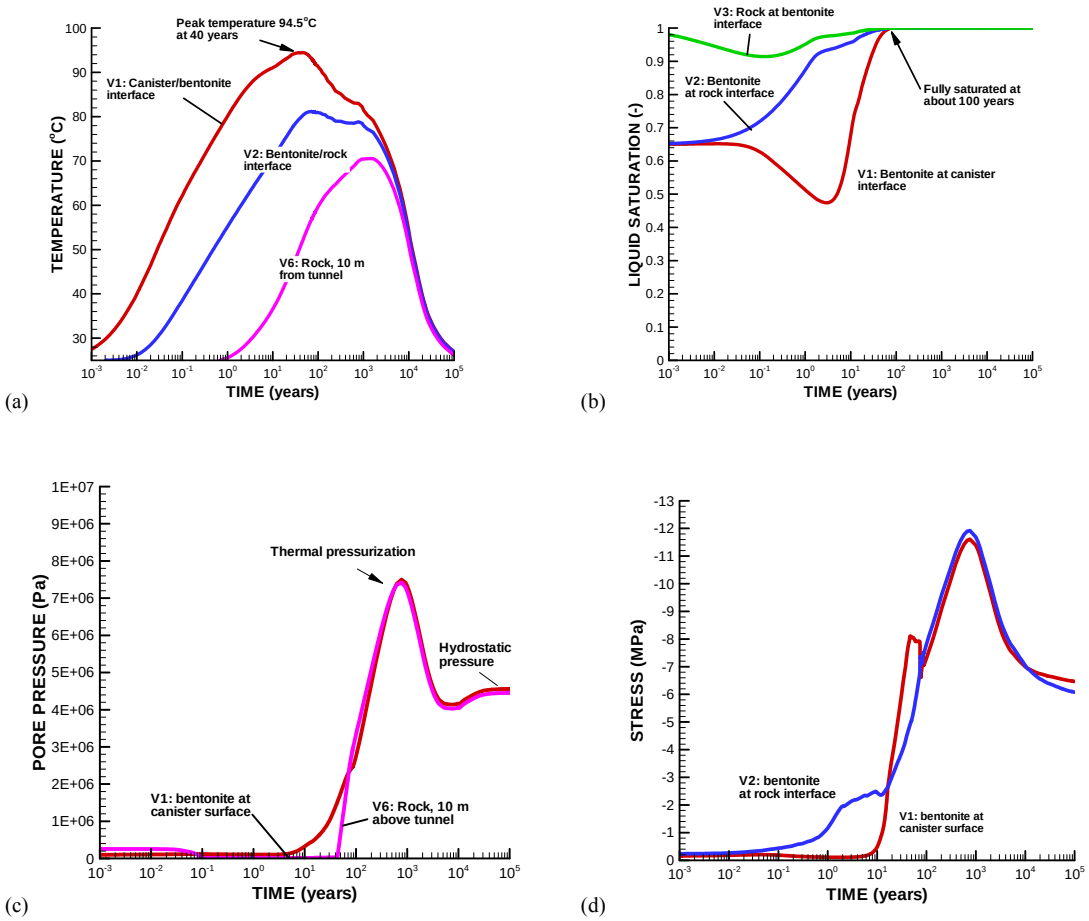

Figure 2.2. Simulated evolution of THM processes in buffer: (a) temperature, (b) liquid saturation, (c) fluid pressure, and (d) total radial stress (σx). See Figure 2.1 for locations of V1, V2, V3, and V6.

Figure 2.3 presents the evolution of total and effective stresses near the tunnel wall (V3 in Figure 2.3a) and 10 m away from the tunnel (V6 in Figure 2.3b). Figure 2.4 shows the profound effect of pressurization on the effective stress evolution; it specifically shows the resulting effective stress path (σ'_1 versus σ'_3) at point V3. The result for the calculated elastic stress path is compared with strength values for the Opalinus clay stone. The range between low and high strength envelopes in Figure 2.4 corresponds to the estimated strength parallel and perpendicular to the bedding planes. This result indicates a high likelihood of failure for the lower strength, parallel to beddings. Such a failure would induce shearing along bedding planes that could lead to increased permeability adjacent to the tunnel, which could impact flow and radionuclide transport should a canister fail.

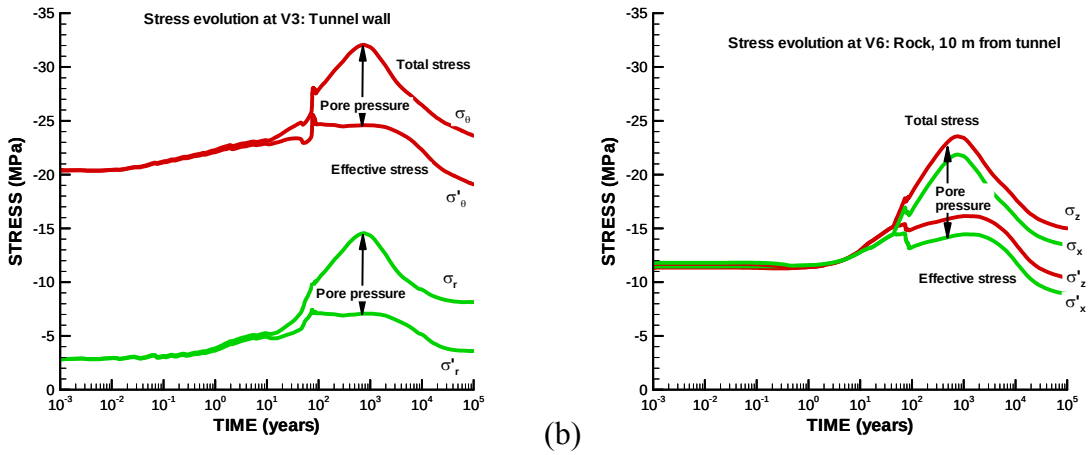

Figure 2.3. Calculated evolution of stresses: (a) stress evolution a point V3 located at the tunnel wall, and (b) stress evolution at point V6 located 10 m away from the tunnel. See Figure 2.1 for locations of V3 and V6.

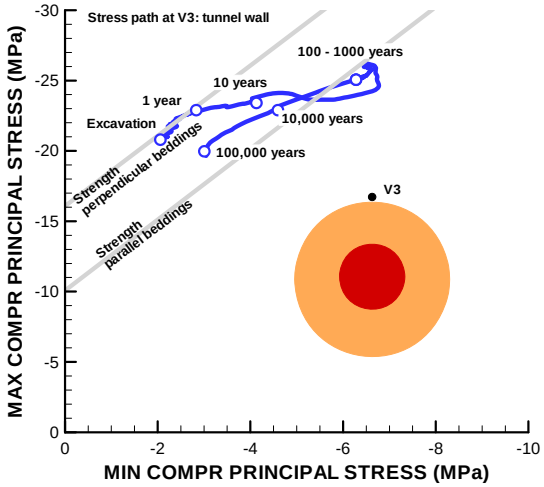

Figure 2.4. Calculated principal stress path at point V3 located at the tunnel wall.

2.2 Thermal management study and peak temperature

The maximum temperature and temperature-time behavior of the canisters are determined principally by the canister and areal thermal loading—which are controllable parameters—and the ambient temperature and thermal properties of the bentonite backfill and rock. There are no strict criteria for establishing a maximum near-field temperature, but it is generally considered that the concerns regarding assurance of good long-term

performance of the bentonite buffer, rather than those associated with corrosion performance of the canister, are the most stringent (NAGRA, 2002). Specifically, the canister surface should be maintained at a sufficiently low temperature that the desirable plasticity and hydraulic and diffusion properties of the buffer material are preserved (NAGRA, 2002). The most important potential degradation processes involve cementation as a result of silica dissolution and precipitation, and precipitation of sparingly soluble salts (e.g., calcite and anhydrite) at or near the canister surface. Several studies have proposed a design with a maximum canister surface temperature of 100°C, because of concerns about bentonite integrity at temperatures above 100°C and because of a lack of confidence in the coupled THM models describing the evolution of near-field conditions over the first few hundred years after emplacement (NAGRA, 2002).

In the Swiss concept for a repository in Opalinus Clay, the maximum surface temperatures for the canister are well above 100°C. Because of the low thermal conductivity of granular bentonite prior to resaturation and the relatively high ambient temperature (38°C) in Opalinus Clay at repository depth, it is difficult to keep temperatures below 125°C throughout the entire bentonite barrier (NAGRA, 2002). In fact, calculations of temperature evolution show that the maximum canister surface temperature will reach ~150°C, and at the point in the bentonite midway between the canister and the tunnel wall, it may reach ~110°C. However, it appears that the more recent studies indicated a maximum temperature of about 125 to 135°C near the canister, which is still substantially above 100°C.

In the previous simulation, we designed the repository in such a way that the peak temperature would be less than 100°C. To achieve this, we assumed a waste deposition after 60 years of interim storage (initial heat power per 1818 W per waste package), deposition at 500 m (initial temperature 25°C), a 50 m tunnel spacing, and canisters emplaced every 8th meter along the emplacement tunnels. Here, we present sensitivity-test results for the parameters related to peak temperature.

Buffer saturation and thermal conductivity: A low buffer saturation and associated low thermal conductivity are mentioned as reasons for the high peak temperature in the Swiss repository concept in Opalinus clay. If buffer is emplaced using granular bentonite, the initial water content is low, leading to a low thermal conductivity (0.4 W/mK). In our simulation, we tried to vary initial saturation between 1% and 100%. A 1% buffer saturation corresponds to the current concept for the Swiss repository in Opalinus clay when using granular (pellets of) bentonite buffer. The results indicate that a change in initial saturation affects the temperature during the first 10 years, before any significant wetting of the buffer from the surrounding rock. As long as the initial saturation is higher than about 10%, the peak temperature is close to 94.5°C and occurs at about 40 years from waste emplacement. If initial saturation is less than 10%, an earlier temperature peak appears at about 2 years after waste emplacement. For the extreme case of a 1% initial saturation, the maximum temperature at the first peak is about 103.5°C, while the maximum temperature at the second peak remains at about 94.5°C (Figure 2.5).

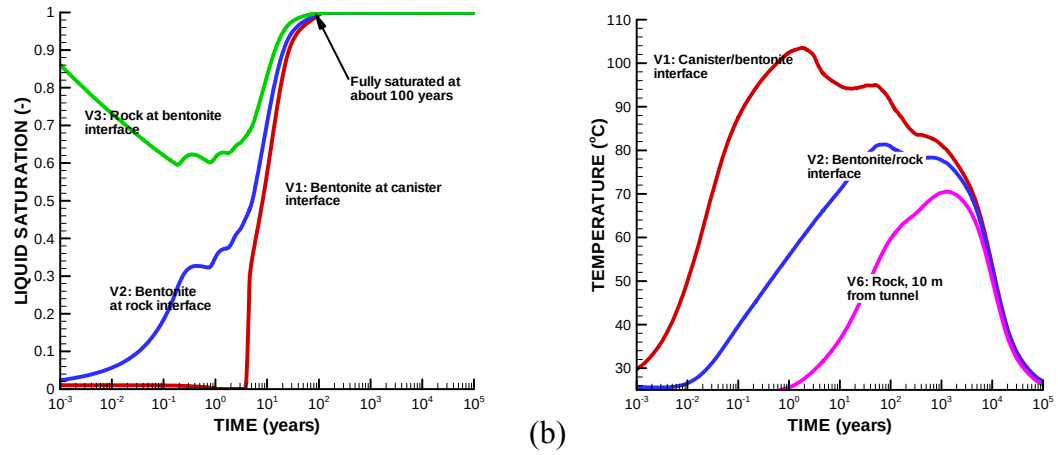

Figure 2.5. Calculated evolution of (a) liquid saturation and (b) temperature in the case of a buffer consisting of granular bentonite with 1% initial saturation.

Tunnel and canister spacing: Both tunnel and canister spacing will impact the temperature evolution. A change in canister spacing will affect the thermal line load along the axis of the emplacement tunnels. In the base case, the canisters containing four-PWR elements were assumed to be 4 m long and spaced 4 m apart. When we reduced the space between the canisters from 4 to 3 m (i.e., a canister every 7 m), the peak temperature increased to 104.2°C at 40 years. When reducing the distance between emplacement tunnels to 35 m, the temperature peaks at about 104.5°C at 60 years.

***Rock thermal conductivity*:** In the base-case scenario, we assign an average thermal conductivity of 2.2 w/mK. This was the average value based on anisotropic thermal conductivity back-calculated from field experiments at Mont Terri, Switzerland. If we reduce the thermal conductivity to the lowest value of 1.6 W/mK, the calculated maximum temperature is about 108°C at 40 years.

***Extreme case of high peak temperature*:** We present the results for an extreme case with low initial buffer saturation, canisters placed every 6 m along the tunnels, and individual tunnels spaced 35 m apart (Figure 2.6). The low buffer saturation also results in a low thermal conductivity. Moreover, we used the lower limit thermal conductivity of rock (1.6 W/mK). The temperature evolution at the canister surface has two peaks: Peak 1 is caused by saturation dependent thermal conductivity of buffer, whereas peak 2 dependents on host rock thermal conductivity and tunnel spacing etc. The peak temperature in this case is much too high.

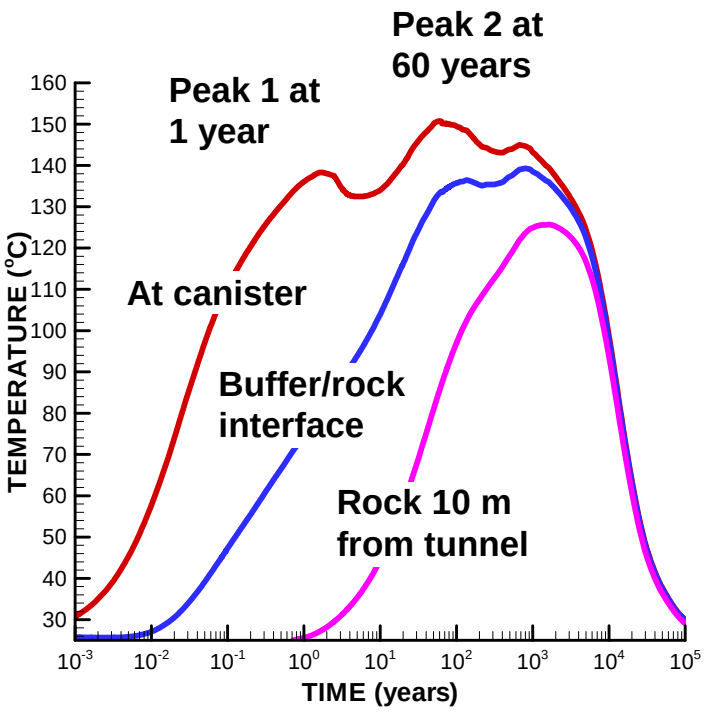

Figure 2.6. Calculated temperature evolution for the extreme case densely spaced waste canisters (reduced canister and tunnel spacing) and a buffer consisting of granular bentonite with 1% initial saturation, as well as a low thermal conductivity of the rock.

2.3 Resaturation time and buffer swelling

The bentonite buffer will resaturate and swell with inflow from the surrounding rock mass. A certain swelling pressure will assure buffer homogeneity and tightness against the surrounding rock wall. The time to full resaturation and swelling depends on a number of parameters, most importantly the hydraulic properties of the rock and the bentonite. We found in our previous simulation that the resaturation time is about 100 years, assuming an average permeability of 5×10^{-20} m^2. The 100-year resaturation time does not change significantly with the different options of heat load or initial saturation of the buffer.

We conducted a parameter study in which we varied the rock permeability and noted the time to reach 99% saturation at the canister surface. Figure 2.7 shows that for the base case, the exact time to 99% saturation is 55 years. If the permeability is one order of magnitude lower (i.e., k = 5×10^{-21} m^2), the resaturation time increased to 177 years. Increasing rock permeability by one order of magnitude results in a decrease in resaturation time to 26 years. Figure 2.7 also shows that if rock permeability were higher than about 1×10^{-16} m^2, the resaturation time is 16.7 years and independent of the rock-mass permeability.

Next, we investigated the sensitivity of the rock water retention and relative permeability functions to the evolution of saturation. In the base case, van Genuchten water retention parameter P_0 = 48 MPa. When decreasing P_0 from 48 to 4.8 MPa for the rock, we can see that the resaturation time increased slightly, from 55 to 65 years, and that there was a more substantial desaturation of the host rock. This desaturation results from high suction in the bentonite at its initial saturation of 65%. A change in the relative permeability function of the host rock had only a minor impact on the resaturation time. Initially the rock is fully saturated while the buffer is 65% saturated at high suction. A strong pressure gradient from the host rock to the bentonite results in fluid flow from the host rock to the buffer. This results in desaturation of the host rock (See point V3 in Figure 2.2b). In the case of a lower P_0 for the host rock, the saturation is lower for a given suction.

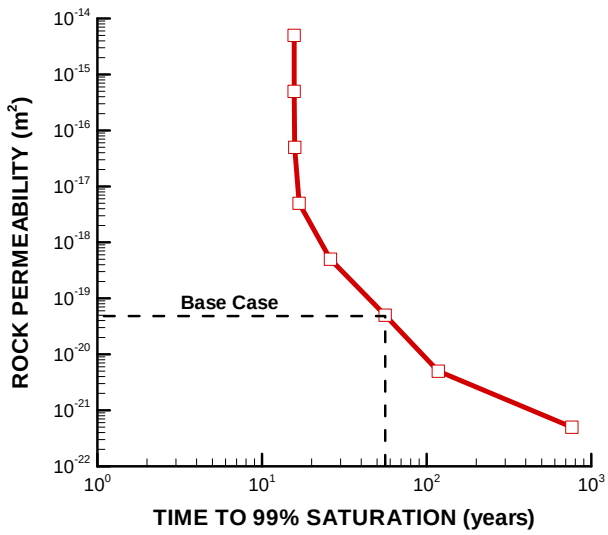

Figure 2.7. Time to 99% saturation for different values of rock-mass permeability.

2.4 Rock failure for layered rock

In this case, we introduced the anisotropic strength properties of the host rock. We used the ubiquitous joint model available in FLAC3D along with the properties shown in Table 2-4—the values used are taken from Gens et al. (2007). Here, we utilize the FLAC3D ubiquitous joint model, a model also used by Corkum and Martin (2007) when simulating previous *in situ* experiments in Opalinus clay at Mont Terri. We assumed that the bedding planes are parallel to the tunnel and slightly tilted (20°). We ran this simulation for base-case properties (except for rock mass).

The results of the simulation using the anisotropic strength properties are shown in Figures 2.8 and 2.9. Figure 2.8 shows volumetric and shear strain induced during the operation and post-closure periods of the repository until 100,000 years. We can observe the anisotropic strain pattern in which most strain occurs near the top and bottom of the

tunnel. Actually, most of the rock mass failure around the tunnel occurs already during the excavation. As shown in Figure 2.9, the stress after excavation is already on the failure envelop for the assigned strength properties. During subsequent waste emplacement and heating of the rock mass, the stress path moves away from failure and the volumetric and shear stresses are quite small. The development of the swelling pressure in the buffer can prevent further rock failure from occurring. The stress path in Figure 2.9 looks similar to that in Figure 2.4, but the maximum compressive principal stress is shifted to a smaller level in Figure 2.9. Note that the simulation results presented in Figure 2.4 was for elastic stress in an elastic medium, whereas the results in Figure 2.9 includes full elasto-plastic analysis with stress response to failure.

Table 2-4. Material properties of the ubiquitous joint model.

Property	**Value**
Bulk modulus	4.17 GPa
Shear modulus	1.92 GPa
Cohesion	5 MPa
Friction angle	25°
Dilation angle	10°
Tensile strength	1.0 MPa
Joint cohesion	2.2 MPa
Joint friction	25°
Joint tensile strength	0.5 MPa

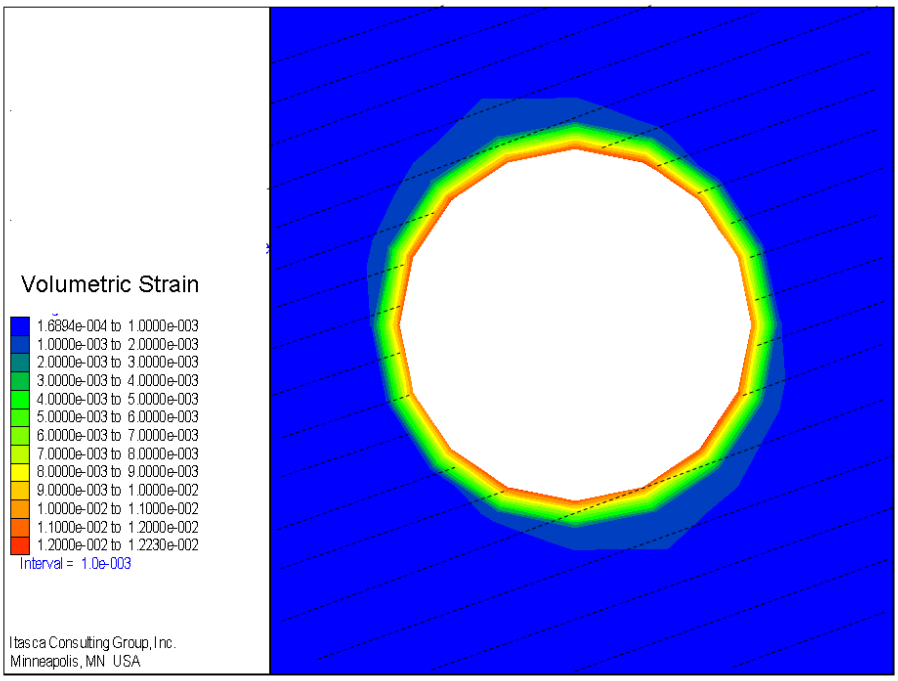

(a)

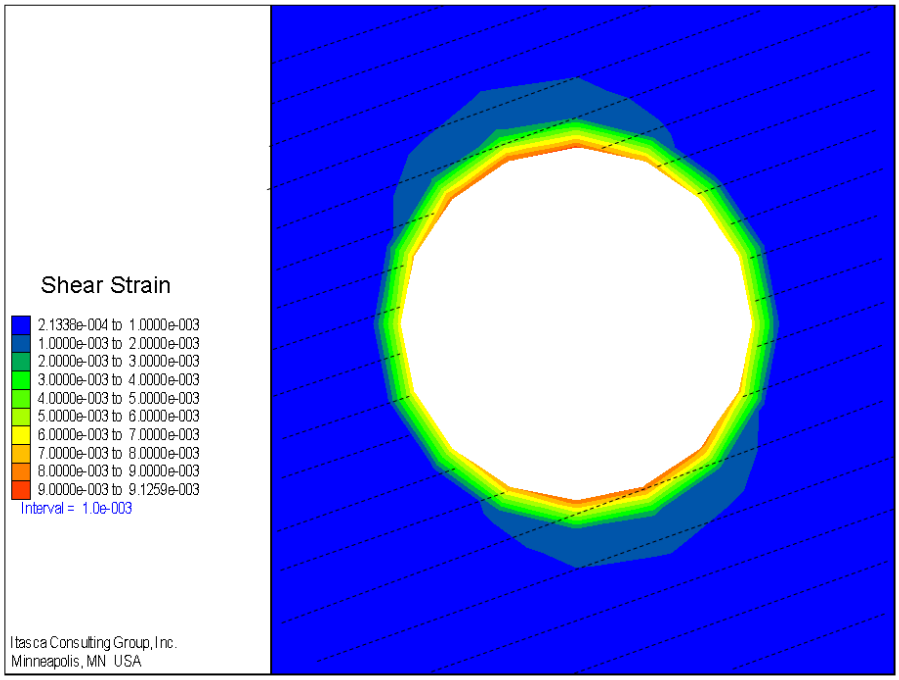

(b)

Figure 2.8. (a) Volumetric strain and (b) shear strain in the rock at 100,000 years for the case of anisotropic strength properties (the orientation of the bedding planes are indicated).

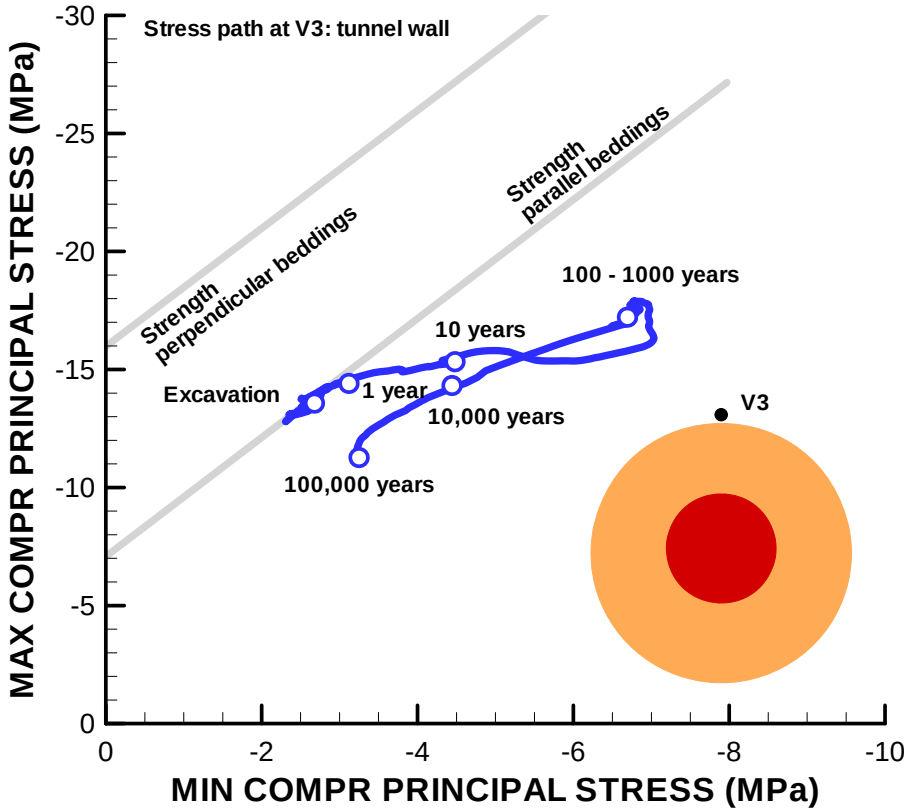

Figure 2.9. Calculated stress path for the case of anisotropic strength properties of the host rock.

2.5 Model development and code implementation of double-structure constitutive model for bentonite

We have identified an approach and suitable mathematical formulation (Alonso et al., 1999), equivalent to the Barcelona Expansive Model. The formulation is being implemented in C++ routines within the User Defined Model framework of the FLAC3D simulator. Once implemented, it will be verified and tested against published data. For example, Alonso et al. (1999) presents such experimental data and numerical tests. Using this model, we will be able to properly model both the micro- and macrostructure deformations and their interactions. Figure 2.10 shows the interaction between micro and macro-structure deformations in the suction, s, versus effective mean stress, p.

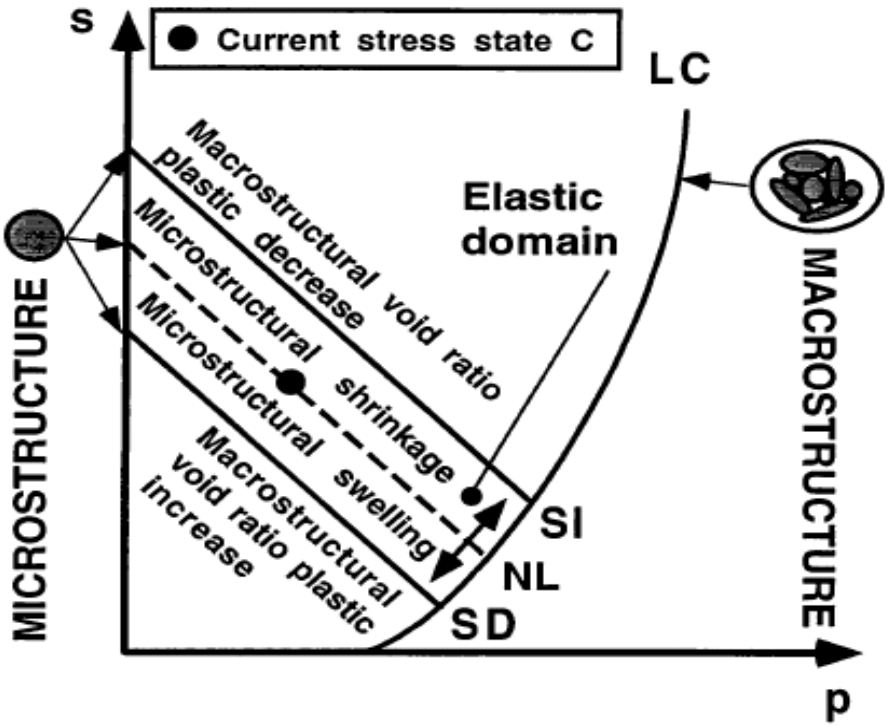

Figure 2.10. Microstructural and macrostrural elastoplastic responses in a double-structure model equivalent to the Barcelona Expansive Model.

3. Reactive Diffusion in Bentonite

Compacted bentonite has been proposed as backfill material in many of the European repositories, because of its very low permeability (Kim et al., 1993; Muurinen, 1994; Pusch, 2001; Bourg et al., 2003) and its strong sorptive properties (Ochs et al., 2001), both of which will limit the release of radionuclides. The low permeability of bentonite is largely due to the fact that it contains a high percentage of Na-montmorillonite, a clay that swells in water. The very low permeability of the compacted bentonite implies that transport of radionuclides away from the waste forms will be almost exclusively by molecular diffusion, with effective diffusivities far below that in water (Madsen, 1998; Ochs et al., 2001; Bourg et al., 2007). Effective diffusivities for the compacted bentonite are very low as a result of its low porosity and the nanometer scale of the pores in the compacted clay. In much of the compacted bentonite, the pores are so small (<1 nanometer) that the electrical double layers balancing the charge of the bentonite (typically negative at circumneutral pH) overlap, thus potentially excluding anions altogether, or creating a deficiency in them with the diffuse double layer balancing the surface mineral charge (Bourg et al., 2003; Bourg et al., 2006; Leroy et al., 2006; Gonçalvès et al., 2007).

Three types of water presence are recognized in compacted bentonite (Bourg et al., 2003; Wersin et al., 2004):

1. Interlayer water (φ_{IL}) with only water and cations within the Tetrahedral-Octahedral-Tetrahedral (TOT) layers of the montmorillonite. Here, the cations balance the fixed charge of the TOT layers;

2. Diffuse double layer (φ_{DDL}) containing cations and anions, but with an excess of ions (normally cations) to balance the charge of the clay surface;

3. Bulk or free pore water (φ_B), which is charge balanced.

The proportions of each kind of water depend on the compaction of the bentonite, but also the ionic strength through its effect on the width of the diffuse double layer. In addition, the nature of cation affects the swelling and therefore the interlayer spacing.

In this progress report, we focus on using the newly developed explicit diffuse double layer capability in CrunchFlow, along with analytical solutions that apply to the binary salt case, to attempt a predictive continuum model for diffusion through compacted bentonite. Also compared to our model is the "ion equilibrium" approach of Birgersson and Karnland (2009), which is based on a single porosity within the clay interlamellae.

3.1 Experimental investigation of diffusion through compacted bentonite

Van Loon et al. (2007) performed a set of through-diffusion experiments in the experimental setup shown in Figure 3.1 using $^{36}Cl^-$ as a tracer and varying the dry density of bentonite and the ionic strength of the saturation solution.

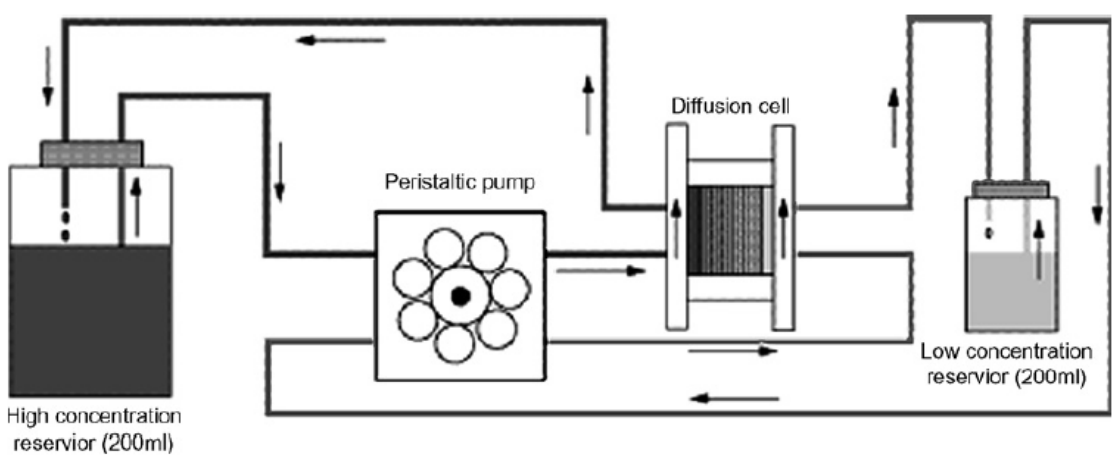

Figure 3.1. Schematic view of the experimental setup used in the through-diffusion experiment (from Van Loon et al., 2007).

The authors attempted to analyze through-diffusion experiments within the framework of the classical theory of molecular diffusion in porous media, using the well-known Fick's law, as given by the following equation valid for one-dimensional cases:

$$\frac{\partial C}{\partial t} = D_e \frac{\partial^2 C}{\partial x^2} \tag{3.1}$$

where D_e represents the effective diffusion coefficient, C is the concentration of a given species and t and x are time and space, respectively.

Under steady-state conditions, the accumulated mass of the tracer is given by the following expression:

$$A(L,t) = SLC_0\left(\frac{D_{eVL}t}{L^2} - \frac{\alpha}{6}\right) \tag{3.2}$$

where S is the cross-sectional area, L is the length of the sample, and C_0 is the concentration of the tracer in the high concentration reservoir. Here it is assumed that concentrations in the "low concentration" reservoir are equal to zero.

The values of D_{eVL} (the effective diffusion coefficient as defined by Van Loon et al., 2007) and α can be obtained graphically by plotting the measured values of $A(L,t)$ against time.

In turn, the rock capacity factor is defined as:

$$\alpha = \phi + \rho_b R_d \tag{3.3}$$

where ρ_b is the bulk dry density and R_d is the distribution coefficient of clay. If nonsorbing tracers are involved, then $R_d = 0$ and $\alpha = \phi$. In the identity above, the porosity ϕ refers to the pore space available to the tracer in question, and thus is strictly true whenever anion exclusion or, more generally, surface processes can be neglected. Otherwise, as is the case here, a distinction should be made between the total volume of pores and the smaller one that is effectively accessible to chloride. The obvious drawback of the so-defined chloride-accessible porosity, ε_{Cl^-}, is that its correspondence with a measurable physical entity is necessarily vaguer than is the case for the total porosity, ϕ. On the other hand, it is not entirely correct to assume that the measured chloride concentration at the outlet is uniformly distributed over the accessible porosity. Rather, it is strictly correct to state that a function of distribution of concentration with respect to space, $C(x,y,z)$, exists, such that:

$$\int_{\phi V_T} C(x,y,z)\,dV = \left[Cl^-\right]\varepsilon_{Cl^-}V_T \tag{3.4}$$

where V_T is the total volume of the sample.

In fact, the derivation of the actual form of the function $C(x, y, z)$ is one of the keys to the solution of the problem and will be dealt with in the following.
Furthermore, as a consequence of assuming that the concentration gradient should be calculated on the basis of the difference in tracer concentration between the upstream and downstream reservoirs, the effective diffusion coefficient was found to vary as a function of both the dry density of clay and the ionic strength of the solution. This is in conflict with the traditional Fickian formulation, according to which the effective diffusivity is a property of the porous medium only. Mathematically, this is explicitly accounted for by the traditional definition of the effective diffusion coefficient:

$$D_e = \tau D_0 \tag{3.5}$$

where the diffusion coefficient in pure water, D_0, is corrected by the tortuosity of the porous network, τ.

As a matter of fact, the authors found that the effective diffusion coefficient defined using the two external reservoirs decreases at higher dry densities and at lower ionic strength values. Table 3-1 shows the values reported in Van Loon et al. (2007).

Table 3-1. Effective diffusion coefficients reported by Van Loon et al. (2007) as a function of dry density of clay and sodium chloride concentration in the pore water.

Dry density (kg/m3)	NaCl (M)	Effective diffusion coefficient (m^2/s)
1300	0.01	2.60E-12
1300	0.05	7.50E-12
1300	0.10	1.60E-11
1300	0.40	2.50E-11
1300	1.00	4.90E-11
1600	0.01	3.90E-13
1600	0.05	1.10E-12
1600	0.10	2.30E-12
1600	0.40	4.60E-12
1600	1.00	1.00E-11
1900	0.01	3.30E-14
1900	0.05	1.20E-13
1900	0.10	2.40E-13
1900	0.40	5.00E-13
1900	1.00	1.20E-12

Glaus et al. (2007), on the basis of diffusion tests carried out in highly compacted clay columns with $^{22}Na^{+}$ and $^{85}Sr^{2+}$ as tracers, removed the ambiguity associated with a formulation based purely on the two ("upstream" and "downstream") reservoirs by postulating that effective diffusion coefficients are independent of the composition of the

external aqueous phase, if the concentration gradient in the interlayer water of the clay is considered. The internal concentration gradient should vary consistently as a function of the external salt concentration.

Figure 3.2 shows that the variation in the effective diffusion coefficient, as calculated from the concentration gradient in the external aqueous phase, does vary with the ionic strength of the saturation solution. That variation can nevertheless be evaluated using a function of the form:

$$D_{eVL} = f\left(D_e, CEC, [A]^{-z}\right) \tag{3.6}$$

where D_e is the actual effective diffusion coefficient of clay, CEC is its cation exchange capacity, $[A]$ is the cation concentration in the external water phase and z is the valence of the tracer. Plotted on a logarithmic scale, experimental points align along a line with slope $-z$, which is -1 for $^{22}Na^{+}$ and -2 for $^{85}Sr^{2+}$.

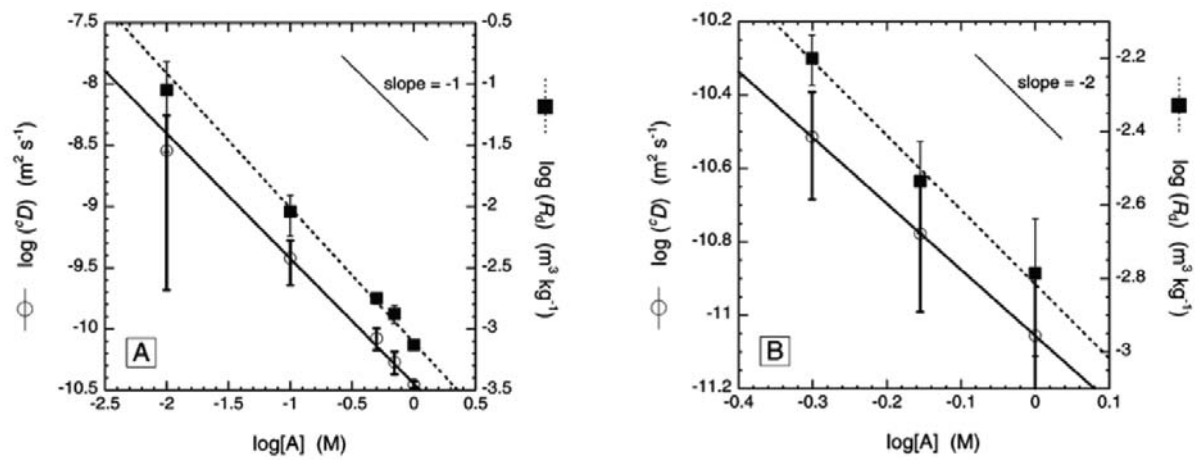

Figure 3.2. Logarithmic representation of the dependence of ^{c}D and Rd for $^{22}Na^{+}$ (Plot A) and $^{85}Sr^{2+}$ (Plot B) on the cation concentration in the external water phase [A]. The data are mean values of results from through-diffusion experiments and profile analysis; 5 mm and 10 mm clay thickness (from Glaus et al., 2007).

3.2 Single type pore model

It is then apparent that, just as diffusion through the interlayer water becomes the dominant pathway, surface reactions between the aqueous phase and the clay become an increasingly relevant factor to consider. As discussed above, all experiments were performed in highly compacted clays (dry density being ~1950 kg/m^3) and therefore conclusions derived from that study could only be applied under similar conditions. These conditions motivated Birgersson and Karnland (2009) to develop their own model. In line with the notion that the effective diffusion coefficient should be independent of the external salt concentration, the authors explicitly account for the distortion of the concentration gradient in the interlayer (with respect to the gradient established between

the inlet and outlet reservoirs) by assuming that Donnan equilibrium relationships hold when applied to the interface between the external and pore solutions. Indeed, anion concentration drops while cation concentration rises at the interfaces, as shown in Figure 3.3.

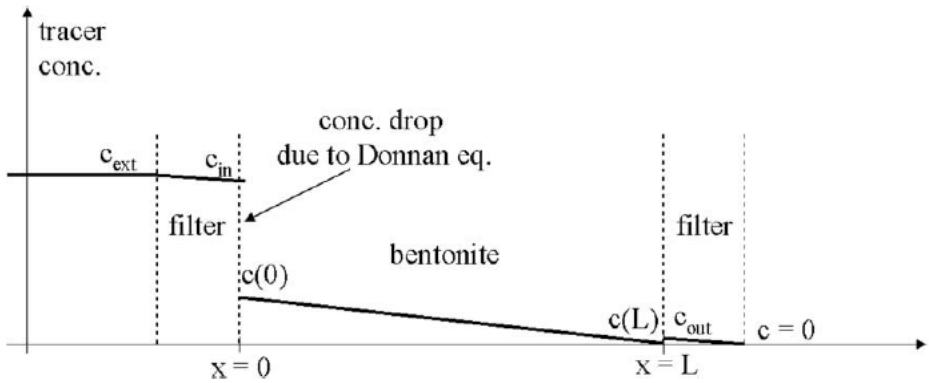

Figure 3.3. Tracer concentration profile at steady state for chloride through-diffusion. For typical experimental setups, the transport capacity of the filters is large enough to supply the clay with anions, and the full concentration drop occurs within the clay. Thus, filters do not need to be considered for evaluation of clay chloride diffusivity (from Birgersson and Karnland, 2009).

These effects can be quantified in terms of the ratio between the concentrations of the tracer in the pore solution and in the external solution (explicitly given for a case where chloride is used as a tracer):

$$\Xi_{Cl^-} = \frac{\left[Cl^-\right]^{MP}}{\left[Cl^-\right]} \tag{3.7}$$

where $\left[Cl^-\right]$ represents the concentration of chloride in the external solution and superscript MP stands for microporosity. This notation implies that, at such high levels of compaction, the entire volume of water in clay pores is affected by the surface charge, i.e., the thickness of the pores is such that the diffuse double layer fully occupies it (hence the term "single type pore model" often employed by the authors). In other words, the function of distribution of concentration over the pore space is $C(x,y,z) = \left[Cl^-\right]^{MP}$, for any point (x,y,z) lying in the pore space (Figure 3.4). This is a debatable assumption, and its consequences will be discussed later.

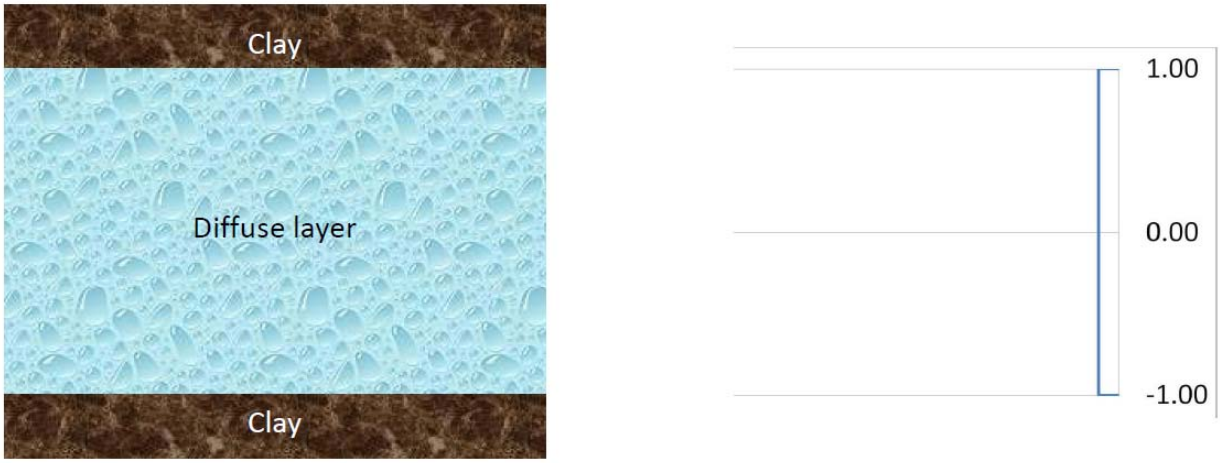

Figure 3.4. Spatial distribution of concentration of chloride as modeled by Birgersson and Karnland (2009).

In the following, the mathematical expression of Ξ_{Cl^-} will be derived on the basis of Birgersson and Karnland (2009) for a simple case involving a solution of sodium chloride. Moreover, it will be demonstrated that it corresponds to a special case of a more general problem that CrunchFlow is able to handle.

Let $\left[Na^+\right]^{MP}$ and $\left[Cl^-\right]^{MP}$ be the concentration of sodium and chloride in the microporosity; then the Donnan equilibrium constraint reduces to the following relationship:

$$\gamma_{Na^+}\left[Na^+\right]\gamma_{Cl^-}\left[Cl^-\right]=\gamma_{Na^{+MP}}\left[Na^+\right]^{MP}\gamma_{Cl^{-MP}}\left[Cl^-\right]^{MP} \tag{3.8}$$

where $\left[Na^+\right]$ and $\left[Cl^-\right]$ are the concentration of sodium and chloride in the external solution and γ_{X_i} is the activity coefficient of the of the species X_i.

So the problem revolves around the calculation of $\left[Na^+\right]^{MP}$ and $\left[Cl^-\right]^{MP}$ based on the equation above. In a 1:1 electrolyte, as in this case, $\left[Na^+\right]=\left[Cl^-\right]$, so:

$$\left[Cl^-\right]^{MP}=\frac{\gamma_{Na^+}\gamma_{Cl^-}\left[Cl^-\right]^2}{\gamma_{Na^{+MP}}\gamma_{Cl^{-MP}}\left[Na^+\right]^{MP}}=\Gamma_1\frac{\left[Cl^-\right]^2}{\left[Na^+\right]^{MP}} \tag{3.9}$$

where

$$\Gamma_1=\frac{\gamma_{Na^+}\gamma_{Cl^-}}{\gamma_{Na^{+MP}}\gamma_{Cl^{-MP}}} \tag{3.10}$$

On the other hand, the mean concentration of sodium ions inside the clay is equal to the sum of the layer charge compensating part ($\left[Na^+\right]_0$) and the amount of ions which has entered from the external solution (the latter being equal to $\left[Cl^-\right]^{MP}$ due to electroneutrality), which is to say:

$$\left[Na^+\right]^{MP} = \left[Na^+\right]_0 + \left[Cl^-\right]^{MP} \tag{3.11}$$

Steefel (2010) writes instead:

$$Q^{SL} = \phi^{MP} \sum_{i=1}^{N} z_i C_i^{MP} \tag{3.12}$$

which holds true for the pore solution in the microporosity (ϕ^{MP} represents the microporosity; Q^{SL} the total charge in the Stern layer, that can be calculated in CrunchFlow either dynamically through the surface complexation module, or introduced as a fixed charge in correspondence with the value of CEC; and z_i is the valence of the ions of concentration C_i^{MP}). In the case analyzed, the above equation becomes:

$$Q^{SL} = \phi^{MP} \left(\left[Na^+\right]^{MP} - \left[Cl^-\right]^{MP} \right) \tag{3.13}$$

which is equivalent to Equation (3.11), given that:

$$\left[Na^+\right]_0 = \frac{Q^{SL}}{\phi^{MP}} \tag{3.14}$$

So both formulations will provide identical results in those cases where it can be assumed that the entire porosity is made up of micropores, i.e., $\phi = \phi^{MP}$.

The charge of the Stern layer is provided by sodium counterions and counterbalances the surface charge of clay minerals. In terms of the cation exchange capacity CEC, that results in:

$$\left[Na^+\right]_0 = \left(\frac{CECm_s}{z} \right) / \left(\frac{m_w}{\rho_w} \right) = \frac{CEC}{z} \rho_s \frac{\left(1 - \phi^{MP}\right)}{\phi^{MP}} \tag{3.15}$$

where m_w and V_w are the water mass and volume, respectively; and ρ_w and ρ_s are the specific mass of water and the solid, respectively.

Alternatively, the foregoing equation could be expressed in terms of the surface site density and the specific surface area of clay minerals:

$$\left[Na^+\right]_0 = \frac{\rho_{site} A_{spec} MW_m \phi_m}{V_m} \tag{3.16}$$

where ρ_{site} represents the surface density (in mol/m^2), A_{spec} is the specific surface area (in m^2/g), MW_m is the molecular weight of the mineral (in g/mol) and ϕ_m and V_m are the volume fraction (per unit fluid volume, dimensionless) and the molar volume of the mineral (cm^3/mol).

Therefore:

$$\left[Na^+\right]^{MP} = \frac{\rho_{site} A_{spec} MW_m \phi_m}{V_m} + \left[Cl^-\right]^{MP} \tag{3.17}$$

and later:

$$\left[Cl^-\right]^{MP2} + \frac{\rho_{site} A_{spec} MW_m \phi_m}{V_m}\left[Cl^-\right]^{MP} - \Gamma_1\left[Cl^-\right]^2 = 0 \tag{3.18}$$

Writing

$$\Omega = \frac{\rho_{site} A_{spec} MW_m \phi_m}{V_m} \tag{3.19}$$

The only real solution of the equation is:

$$\left[Cl^-\right]^{MP} = \frac{-\Omega + \sqrt{\Omega^2 + 4\Gamma_1\left[Cl^-\right]^2}}{2} \tag{3.20}$$

Finally:

$$\Xi_{Cl^-} = \frac{\left[Cl^-\right]^{MP}}{\left[Cl^-\right]} = \frac{-\Omega + \sqrt{\Omega^2 + 4\Gamma_1\left[Cl^-\right]^2}}{2\left[Cl^-\right]} \tag{3.21}$$

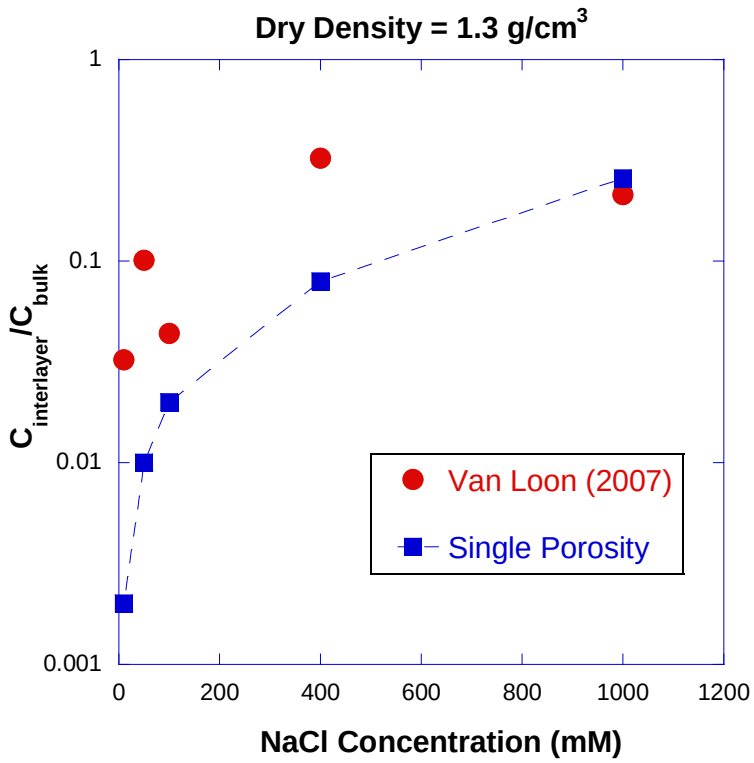
Dry Density = 1.3 g/cm3
1
0.1
0.01
0.001
0
200
400
600
800
1000
1200
C interlayer /C bulk
NaCl Concentration (mM)
Van Loon (2007)
Single Porosity

(a)

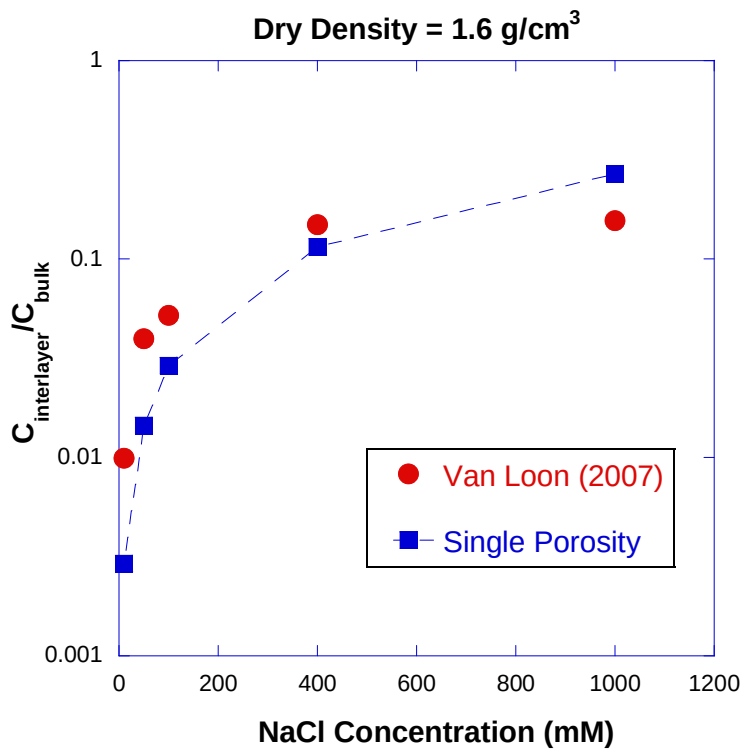
Dry Density = 1.6 g/cm3
1
0.1
0.01
0.001
0
200
400
600
800
1000
1200
C interlayer /C bulk
NaCl Concentration (mM)
Van Loon (2007)
Single Porosity

(b)

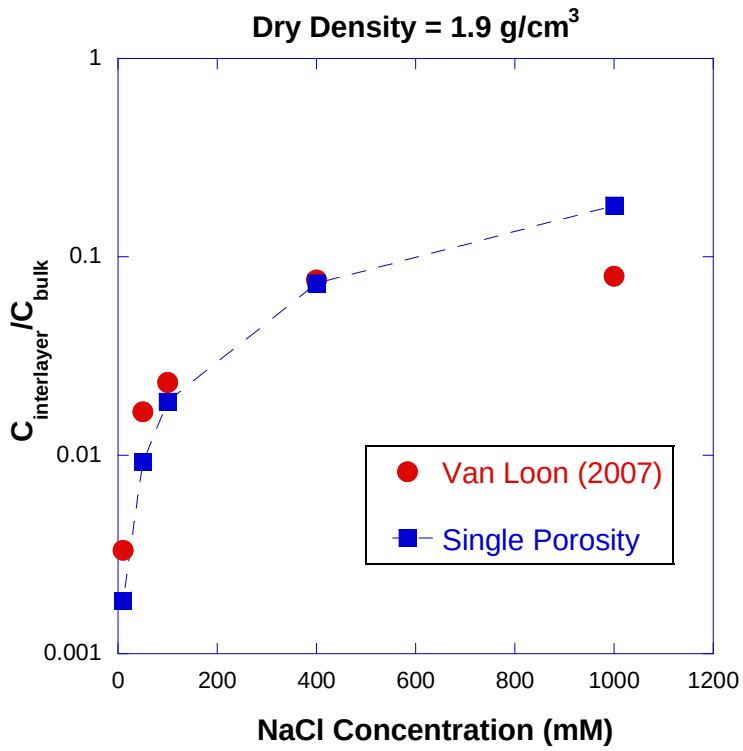

(c)

Figure 3.5. Fit of experimental data reported by Van Loon et al. (2007) obtained by the single type pore model: (a) 1300 kg/m^3, (b) 1600 kg/m^3, (c) 1900 kg/m^3

In Figure 3.5, the results of the model are plotted against the values obtained from through-diffusion experiments carried out by Van Loon et al. (2007) for dry densities equal to 1300 kg/m^3 (a), 1600 kg/m^3 (b) and 1900 kg/m^3 (c). As can be seen, the results of the model match accurately the trend of the ratio observed against both dry density of the clay and ionic strength of the solution. It is apparent, however, that the agreement between model simulations and experimental results is closer as dry density increases. Setting aside experimental errors (Van Loon et al., 2007) estimated the value of ε_{Cl^-} by means of four different methods and some scatter is observable), divergences arising at lower dry densities appear to hint at a limit to the range of applicability of the Birgersson and Karnland model. In other words, the hypothesis underlying the single type porosity model holds strictly true when the pore space is small enough (in correspondence with a high rate of compaction and dry density), while it becomes increasingly questionable as porosity increases, thus allowing for the coexistence of the double diffuse layer, on the one hand, and bulk water, where anion concentrations are much larger, on the other hand.

3.3 Double type pore model

The new capabilities included in CrunchFlow and detailed in Steefel (2010), in line with analytical developments reported in Appelo et al. (2008), allow for the treatment of more complicated scenarios than those considered by the single porosity formulation of

Birgersson and Karnland (2009). Yet it remains to be seen how effective they are in simulating the response of clay as shown above.

It is clear that additional constraints had to be met in developing a more sophisticated and comprehensive model. Indeed, even for the very simple problem outlined above (a clay column saturated with a binary solution and subjected to a slight concentration gradient), the number of unknowns doubles. For the problem to be solved, the unknown concentrations $\left[Na^{+}\right]^{MP}$, $\left[Cl^{-}\right]^{MP}$, $\left[Na^{+}\right]^{P}$ and $\left[Cl^{-}\right]^{P}$ (where the superscript P refer to macroporosity, as opposed to microporosity) have to be determined.
Let $\left[Na^{+}\right]$ and $\left[Cl^{-}\right]$ be the sodium and chloride concentration of the external solution.
Then, the abovementioned constraints are:

1) Donnan equilibrium condition between external and micropore solutions:

$$\gamma_{Na^{+}}\left[Na^{+}\right]\gamma_{Cl^{-}}\left[Cl^{-}\right]=\gamma_{Na^{+MP}}\left[Na^{+}\right]^{MP}\gamma_{Cl^{-MP}}\left[Cl^{-}\right]^{MP} \tag{3.22}$$

2) Donnan equilibrium condition between micropore and macropore solutions:

$$\gamma_{Na^{+MP}}\left[Na^{+}\right]^{MP}\gamma_{Cl^{-MP}}\left[Cl^{-}\right]^{MP}=\gamma_{Na^{+P}}\left[Na^{+}\right]^{P}\gamma_{Cl^{-P}}\left[Cl^{-}\right]^{P} \tag{3.23}$$

3) Electroneutrality in the macroporosity:

$$\left[Na^{+}\right]^{P}=\left[Cl^{-}\right]^{P} \tag{3.24}$$

4) Charge balance in the microporosity:

$$\left[Na^{+}\right]_{0}=\left[Na^{+}\right]^{MP}-\left[Cl^{-}\right]^{MP} \tag{3.25}$$

Note that imposing Donnan equilibrium between the external water and the macropore solution would be redundant.

The solution is then given by the following set of equations:

$$\left[Na^{+}\right]^{MP}=\frac{\left[Na^{+}\right]_{0}+\sqrt{\left[Na^{+}\right]_{0}^{2}+4\Gamma_{1}\left[Cl^{-}\right]^{2}}}{2} \tag{3.26}$$

$$\left[Cl^{-}\right]^{MP}=\frac{-\left[Na^{+}\right]_{0}+\sqrt{\left[Na^{+}\right]_{0}^{2}+4\Gamma_{1}\left[Cl^{-}\right]^{2}}}{2} \tag{3.27}$$

$$\left[Cl^{-}\right]^{P}=\left[Na^{+}\right]^{P}=\sqrt{\Gamma_{1}\Gamma_{2}}\left[Cl^{-}\right] \tag{3.28}$$

$$\Gamma_2 = \frac{\gamma_{Na^{+MP}} \gamma_{Cl^{-MP}}}{\gamma_{Na^{+P}} \gamma_{Cl^{-P}}} \tag{3.29}$$

Let Γ_3 be defined as:

$$\Gamma_3 = \frac{\gamma_{Na^{+}} \gamma_{Cl^{-}}}{\gamma_{Na^{+P}} \gamma_{Cl^{-P}}} \tag{3.30}$$

Then:

$$\left[Cl^{-}\right]^{P} = \left[Na^{+}\right]^{P} = \sqrt{\Gamma_3}\left[Cl^{-}\right] \tag{3.31}$$

It is relevant here to point out that Equation (3.27) and Equation (3.20) are equivalent, in case the volume of reference for $\left[Na^{+}\right]_0$ is that of microporosity, which further confirms that the Birgersson and Karnland (2009) model represents a special case of a more general problem.

Then let the Debye length be defined as:

$$\lambda_D = \sqrt{\frac{\varepsilon RT}{2F^2 I_c}} \tag{3.32}$$

where ε is the permittivity of the medium, and I_c is the ionic strength of the solution. The Debye length (a function of the electrolyte solution) plays an important role in this context, as it gives a notion of the characteristic length over which the overpotential of the clay walls decays into the bulk. More generally, it can be assumed that a given constant K exists such that the double diffuse layer reaches a distance $\lambda'_D = K / \sqrt{I_c}$ from the clay walls. Beyond that distance, bulk water is found.

Let then the bulk surface area be calculated as:

$$S_{Bulk} = \rho_s A_{spec} \phi_m \tag{3.33}$$

The pore space occupied by the double diffuse layer is:

$$V^{MP} = S_{Bulk} \lambda'_D \tag{3.34}$$

if V^{MP} is less than ϕV_T

It follows that the microporosity is:

$$\phi^{MP} = \frac{V^{MP}}{V_T} \tag{3.35}$$

and the macroporosity becomes:

$$\phi^{P} = \phi - \phi^{MP} \tag{3.36}$$

Therefore, the function of distribution of concentration becomes (Figure 3.6):

$$\begin{cases} C(x,y,z) = \left[Cl^-\right]^{MP}, \ \forall (x,y,z) \in \phi^{MP} \\ C(x,y,z) = \sqrt{\Gamma_3}\left[Cl^-\right], \ \forall (x,y,z) \in \phi^{P} \end{cases} \tag{3.37}$$

Figure 3.6. Spatial distribution of concentration of chloride as modeled in CrunchFlow.

Figure 3.7 shows the results obtained with those hypotheses for the cases considered in Van Loon et al. (2007).

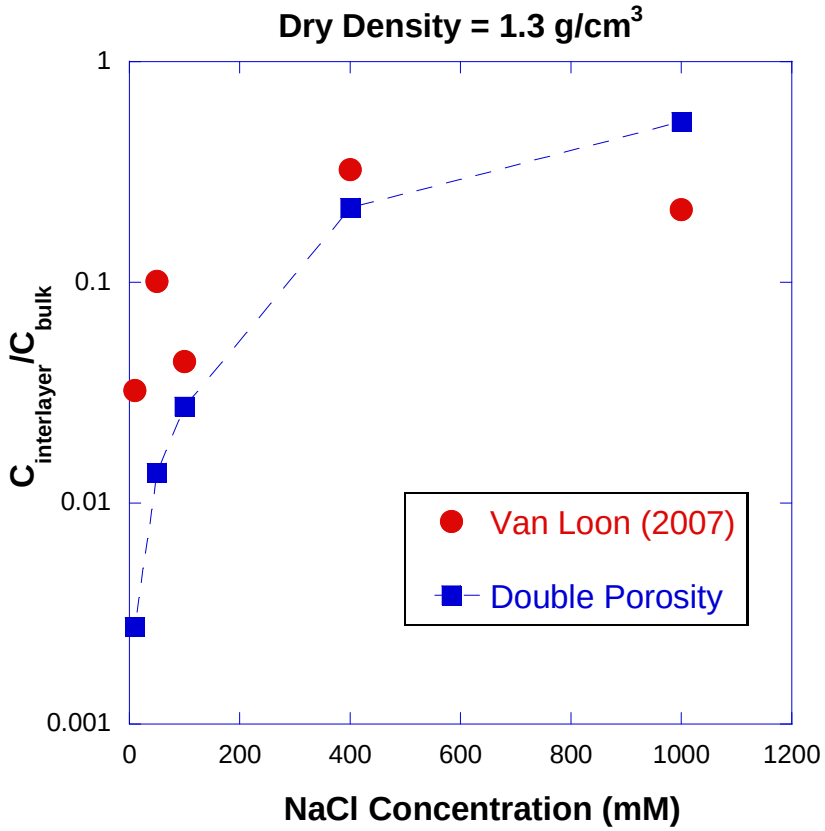
Dry Density = 1.3 g/cm3
1
0.1
0.01
0.001
C interlayer /C bulk
0
200
400
600
800
1000
1200
NaCl Concentration (mM)
Van Loon (2007)
Double Porosity

(a)

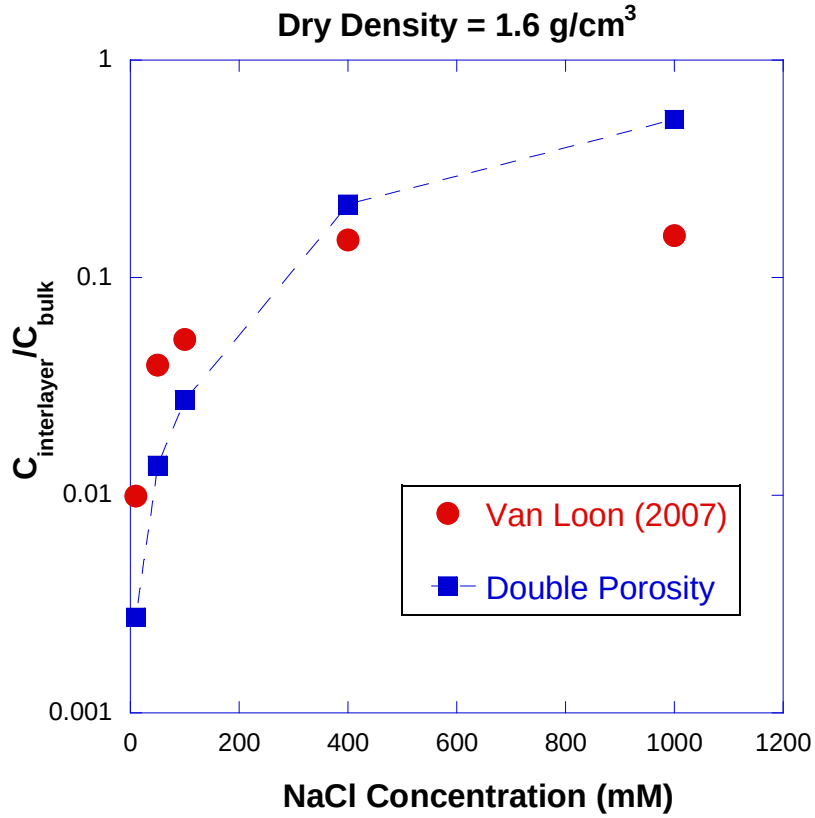
Dry Density = 1.6 g/cm3
1
0.1
0.01
0.001
C interlayer /C bulk
0
200
400
600
800
1000
1200
NaCl Concentration (mM)
Van Loon (2007)
Double Porosity

(b)

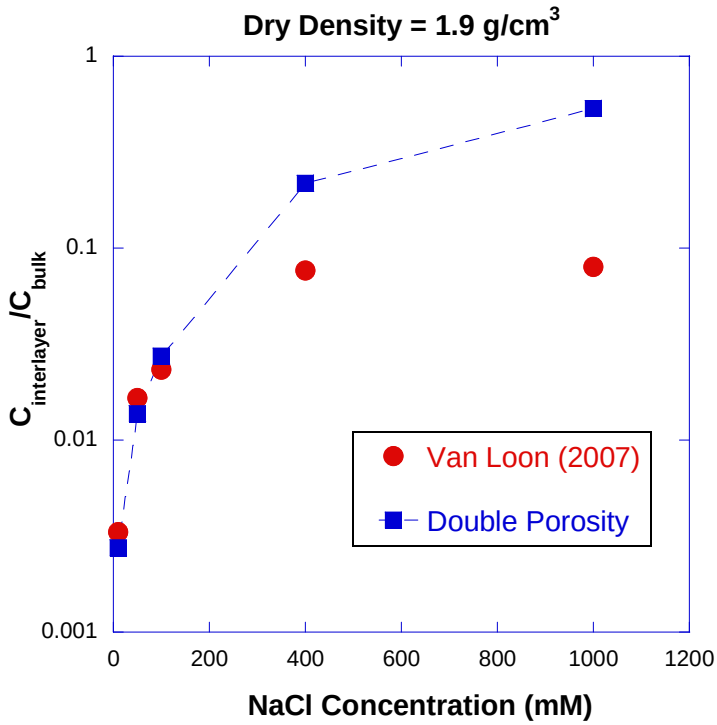

(c)

Figure 3.7. Fit of experimental data reported by Van Loon at al. (2007) obtained by the single type pore model: (a) 1300 kg/m^3, (b) 1600 kg/m^3, (c) 1900 kg/m^3

As can be seen, this approach does not really improve the fit with the Van Loon experimental data on the lower end of the spectrum of ionic strength values considered as compared to the Birgersson and Karnland model. In fact, as ionic strength decreases, the calculated thickness of the double diffuse layer becomes larger up to the point that it occupies the entire pore space, thus replicating the results of the single type pore model. On the higher end, the double type pore model consistently overestimates the actual chloride concentration in the pore water, as the concentration in the bulk water (orders of magnitude larger than that of the double diffuse layer) weighs decisively in the resulting average. All this suggests that, even though allowing for the fact that concentration varies over the pore space, the modeled dual distribution of concentration fails to reproduce the variation in diffusion rates and gradients properly.

3.4 Analytical solution

In view of the conclusions reached thus far, a more sophisticated model is required to evaluate the actual distribution of concentration in the pore space. To that aim, it was deemed useful to approach the problem by attempting to solve the differential equations that describe the spatial distribution of electrical potential and its influence on the concentration of ionic species (Kirby, 2010).

Let the general form of the Poisson-Boltzmann equation be given by:

$$\nabla^2\varphi = -\frac{F}{\varepsilon}\sum_i^N c_{i,\infty} z_i exp\left(-\frac{z_i F\varphi}{RT}\right) \tag{3.38}$$

where $c_{i,\infty}$ represents the concentration of the i-th ionic species in the region of the pore unaffected by the electrical potential of clay walls.

For most practical cases, the Poisson-Boltzmann equation can only be solved numerically. Nevertheless, the problem simplifies significantly when dealing with a binary solution, as in this case. Moreover, if the product $z_i\varphi$ is small enough with respect to unity, the exponential function could be linearized by truncating the Taylor expansion to the second term. Under such conditions, and assuming that clay particles are arranged according to a layered structure, so that the pores resemble the spaces between two parallel plates, the distribution of the electrical potential can be described by:

$$\varphi = \varphi_0 \frac{cosh\left(y/\lambda_D\right)}{cosh\left(d/\lambda_D\right)} \tag{3.39}$$

where φ_0 represents the electrical potential of the shear plane, d is the half-spacing between two layers of clays and y varies between $-d$ and d.
Then, the distribution of chloride concentration as a function over the pore space becomes:

$$C\left(x,y,z\right) = \left[Cl^-\right]^P exp\left[-\frac{zF}{RT}\varphi_0 \frac{cosh\left(y/\lambda_D\right)}{cosh\left(d/\lambda_D\right)}\right] \tag{3.40}$$

where, for the sake of simplicity, the concentration of chloride in the bulk water $\left[Cl^-\right]^P$ was assumed to be equal to the concentration in the reservoir solution (thus neglecting any activity effects), and z (explicitly written here for more general cases) is its valence.
Trial and error was required in order to fit experimental values of Van Loon et al. (2007) by adjusting the variables φ_0 and d for all cases considered. Figure 3.8 shows the profiles obtained for dry densities equal to 1300 kg/m^3 (a), 1600 kg/m^3 (b) and 1900 kg/m^3 (c) with values listed in Table 3-2.

(a)

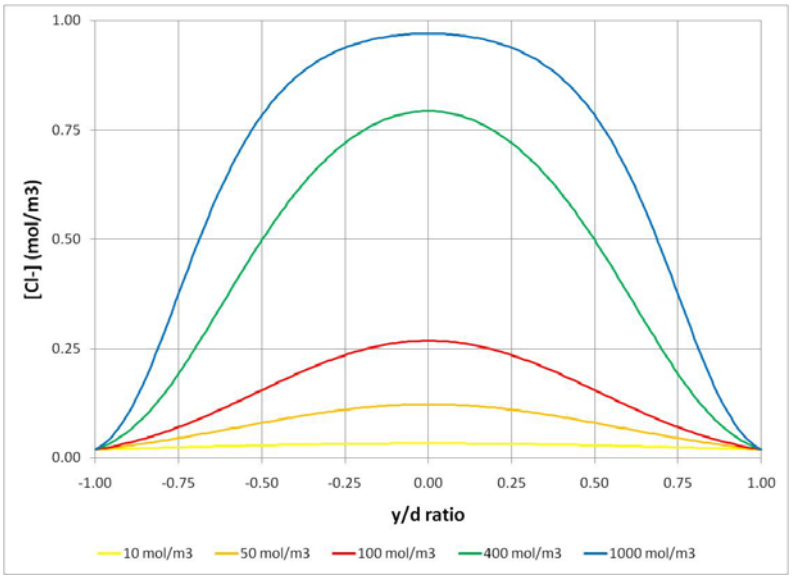
1.00
0.75
0.50
0.25
0.00
[Cl-] (mol/m3)
-1.00
-0.75
-0.50
-0.25
0.00
0.25
0.50
0.75
1.00
y/d ratio
10 mol/m3
50 mol/m3
100 mol/m3
400 mol/m3
1000 mol/m3

(b)

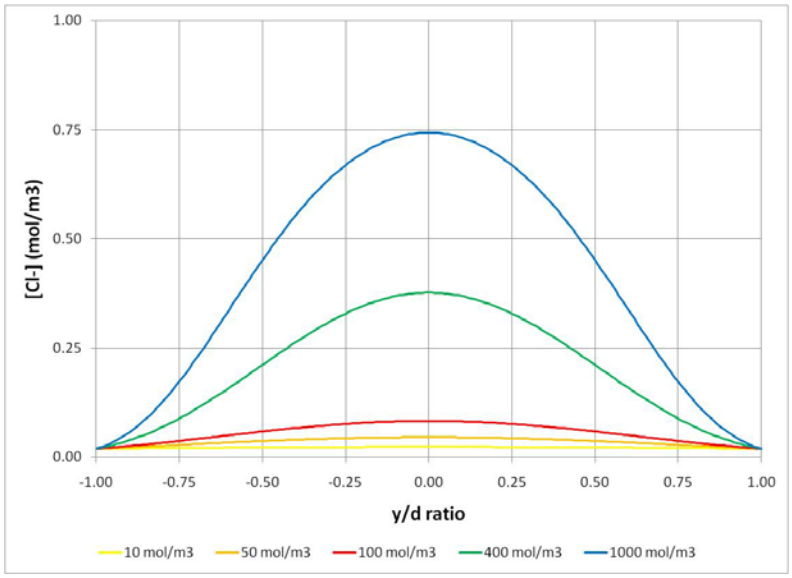
1.00
0.75
0.50
0.25
0.00
[Cl-] (mol/m3)
-1.00
-0.75
-0.50
-0.25
0.00
0.25
0.50
0.75
1.00
y/d ratio
10 mol/m3
50 mol/m3
100 mol/m3
400 mol/m3
1000 mol/m3

(c)

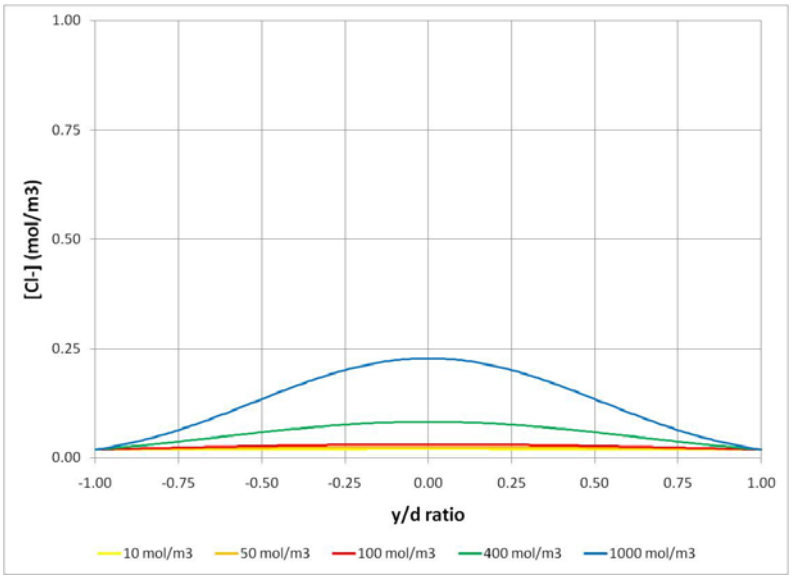

Figure 3.8. Normalized profiles of concentration of chloride obtained with varying ionic strength for a range of dry density values (a) 1300 kg/m^3; (b) 1600 kg/m^3; (c) 1900 kg/m^3.

Table 3-2. Values of electrical potential at the shear plane and of semispacing between clay layers as a function of dry density obtained by fitting procedures of experimental data reported by Van Loon et al. (2007).

Dry density (kg/m^3)	φ_0 **(V)**	d **(m)**
1300	-0.10	1.70E-09
1600	-0.10	1.00E-09
1900	-0.10	5.00E-10

The electrical potential estimated by means of this procedure is significantly higher than that measured by Sondi et al. (1996), as cited in Leroy and Revil (2004), for smectites, which is φ_0 = -0.03 V for a wide range of pH values.

Figure 3.9 shows the fit obtained of the experimental data.

(a)

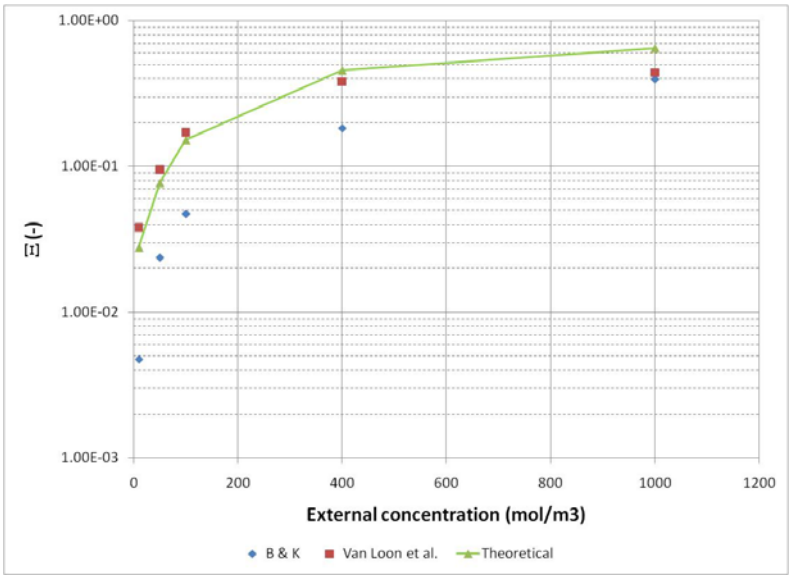
1.00E+00
1.00E-01
1.00E-02
1.00E-03
Ξ (-)
0
200
400
600
800
1000
1200
External concentration (mol/m3)
B & K
Van Loon et al.
Theoretical

(b)

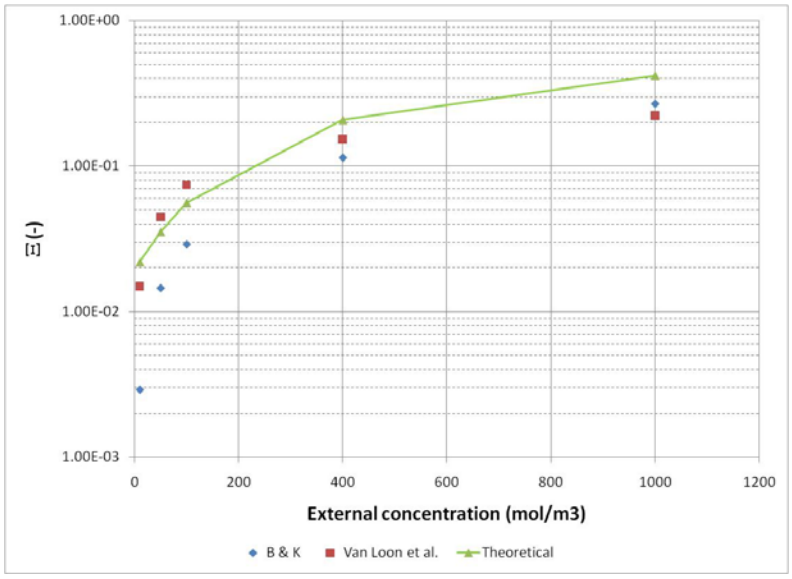
1.00E+00
1.00E-01
1.00E-02
1.00E-03
Ξ (-)
0
200
400
600
800
1000
1200
External concentration (mol/m3)
B & K
Van Loon et al.
Theoretical

(c)

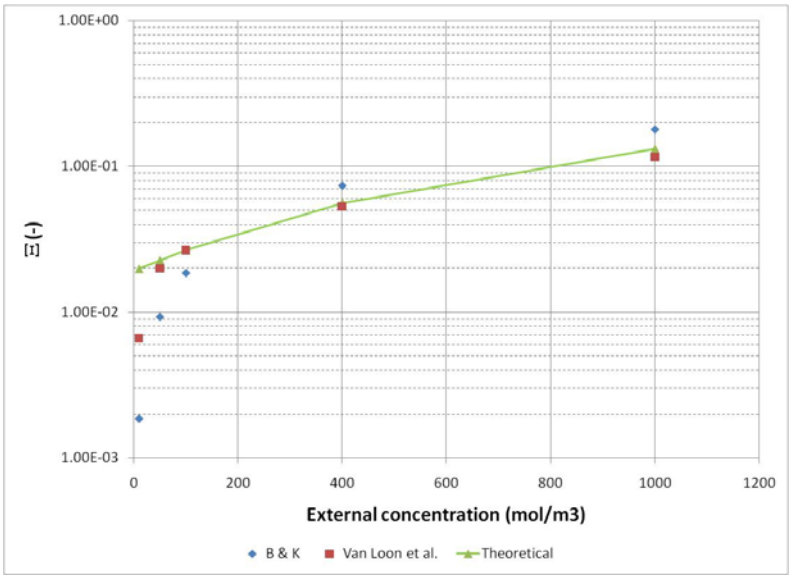

Figure 3.9. Fit of experimental data reported by Van Loon at al. (2007) obtained by the analytical solution of the simplified form of the Poisson-Boltzmann equation for the case of a binary solution between two parallel plates: (a) 1300 kg/m^3; (b) 1600 kg/m^3; (c) 1900 kg/m^3.

The results obtained do not lend themselves to easy interpretation. While for lower dry densities there is acceptably good agreement between modeled and experimental values of Ξ_{Cl^-} at lower ionic strengths, the model tends to overestimate the measured concentration on the other end of the spectrum—Figure 3.9 (a) and (b). On the contrary, the trend reverses completely when dry density is 1900 kg/m^3 (Figure 9 (c)). Several reasons can be invoked to explain these divergences, the most obvious ones being that activity effects might not be negligible and that the actual configuration of the pore space was oversimplified. While this is undeniably true, it is still unclear how these complexities can be incorporated into a suitable model in a practical way, especially as we are moving into the realm of multicomponent diffusion. This remains an open field for further research and is certainly one of the main objectives of this project.

4. Knowledge Gaps and Future Work

4.1 Knowledge gaps

This section reiterates briefly the main knowledge gaps with respect to buffer/backfill and seal performance in a geologic repository (based on Steefel et al., 2010). The list below describes critical technical issues that point to specific R&D needs. An integrated research plan in these areas would involve detailed process-oriented studies, including coupled-processes simulation tools, laboratory experiments, and *in situ* tests.

1. <u>Studies of bentonite hydration to include new processes not included in conventional formulations of THM models</u>. These processes include thermo-osmosis, microstructure evolution, existence of different states of water in the bentonite, and existence of a threshold hydraulic gradient for water flow.

2. Studies of the THM behavior of bentonite pellets and pellet mixtures, and irreversible swelling or compression of bentonite in large gap fillings. This is related to homogenization of the bentonite density in the EBS. Bentonite blocks, pellets, and gaps need to be homogenized to about the same density (heterogeneity to be limited) for bentonite to serve as an effective isolation barrier to radionuclide leakage.

3. Studies of piping and erosion of bentonite. The loss of mass into flowing water needs to be limited. It is further complicated by the localized feature of flow from the host rock. We need to develop conceptual models and computer codes for these processes, as well as experimental data to verify our understanding.

4. Studies of radionuclide transport through bentonite interlayer porosity. By comparing the topics discussed in the literature review and the existing capabilities for modeling of diffusive transport in compacted bentonite, it is clear that a capability for modeling transport through montmorillonite interlayer porosity needs to be developed. In addition, almost no validation of the models has been carried out to date, so this is an important activity that requires effort in the relatively near term.

5. Studies of swelling and self-sealing. While it is well known that swelling and self-sealing exist in both clay buffer materials and clay host rock, well-established model methodologies to deal with these important phenomena and their relations to reactive transport are still lacking in the literature.

6. Studies of gas generation and its modeling. Due to canister corrosion, gas is generated and flows through the EBS (including bentonite) to natural systems (host rock). Gas generation and flow have an important impact on mechanical, chemical, and hydraulic processes in the EBS. [Note that gas flow is relatively sensitive to small-scale heterogeneity.] Although some studies on this topic are available, significant uncertainty remains in this area, in part because models for gas generation and corrosion are decoupled from models for near-field and natural systems behavior. Gas pressure and migration may result in preferential pathways for gas flow and radionuclides that partition into the gas phase. Preferential gas flow along higher-permeability pathways through the EBS could result in fast gas-phase transport to more permeable formations external to the host rock or even the ground surface. Gas flow will also lead to aqueous-phase displacement and aqueous radionuclide transport. Potential cycling of gas flow and rewetting of the bentonite could result in greater aqueous radionuclide transport than possible from a simple single-displacement process.

7. Studies considering explicit interactions between host rock and EBS and between different EBS components. Most previous studies have been focused on detailed understanding/prediction of one or only a few EBS components, while interactions between other components are disregarded or highly simplified (such as waste form interaction with corrosion products and buffer materials). Inclusion of these interactions between different EBS components makes the coupled processes models

more complicated, but at the same time more reliable and usually less conservative. At this point, we are lacking the capability to investigate the interplay between the different components and their interactions via mechanistic process coupling. This interplay may have an important impact on radionuclide release from the EBS. The research described in Section 2 of this report describes studies on the interaction between buffer materials and the near-field host rock.

8. Studies of chemical/mineralogical changes in bentonite. A variety of aqueous chemical and mineralogical changes—including illitization, Na/Ca exchange, reactions with alkaline waters from cementitious materials, reactions with corrosion products, and secondary mineral precipitation—affect mineral volume and mechanical characteristics. The potential for induration of the bentonite through these changes and fracturing caused by changes in mineral volumes, thermal expansion/contraction, volume changes associated with changes in pore-water composition, and volume changes caused by mineral transformations need to be evaluated as part of the chemical/mineralogical evolution of the bentonite. The impact on development of preferential flow and transport channels over long time periods needs to be addressed (Gaucher et al. 2004). The model capability development described in Section 2 of this report will eventually allow incorporation of chemical/mineralogical changes in bentonite behavior.

9. Studies of glass dissolution mechanisms. Evidence indicates that glass dissolution is affected by the presence of bentonite. However, the effects are a complex balance between the dissolved silica concentrations and the solubility limits in the presence of clay. The controls that lead to either a decrease in dissolution rates or continued high dissolution rates in the presence of clays need to be investigated (Houseworth, 2010, Section 2.5; Lemmens 2001).

10. Studies of radionuclide sorption on bentonite for varying conditions, including temperature, pH, Eh, mineral phase (e.g., illitization), and Na/Ca exchange. Numerous observations of sorption indicate varying levels of sensitivity to temperature, pore water, and mineral compositions, depending on radionuclide species. The effects of iron corrosion products on bentonite include increased pH and precipitation of magnetite, which can lead to stronger sorption in the backfill. The large number of potential combinations of conditions and radionuclides means that generating empirical sorption results to cover all potential combinations of conditions and radionuclides is impractical. Therefore, a modeling approach is needed. For this to be successful, thermodynamic databases need to be expanded so that predictions of radionuclide sorption can be made over the range of conditions that may occur. (Houseworth 2010, Section 2.8; Sabodina et al. 2006; Khan 2002; Donat et al. 2005; Samper et al. 2008).

11. Further integration of THM & C models for simulating THMC coupled processes. Significant chemical-mechanical couplings for bentonite mean that the traditional separation of THM and THC coupled processes in most existing software may not be adequate. Given the compatibilities of their software structure, integration of

TOUGHREACT with TOUGH-FLAC as a fully coupled THMC software code is one avenue to consider for attaining this goal. The model capability development described in Section 2 of this report will eventually allow for seamless integration of the reactive transport simulator TOUGHREACT into the TOUGH-FLAC into the TOUGHREACT geomechanical code. Development of a fully coupled THMC capability will be achieved by integration with research activities in the "Repository Science-THCM Near Field" work package.

12. Analysis of recent field data from major experiments studying bentonie behavior. Examples and potential path forwards for gaining access to data from major field experiments are given in Section 5. As discussed therein, some of the data may be found from the published literature or open-access reports, while others are available only through participation in international cooperative projects. Such participation is an effective way to be positioned at the forefront of the state of science in this field.

4.2 Future work in FY11 and FY12

The long-term R&D plans are to develop modeling capabilities, conduct laboratory experiments, and collaborate with international partners to address the technical issues identified above. This subsection presents the work activities in the remaining months of FY11 and in FY12.

THM Modeling

- The double-structure model will be implemented into TOUGH-FLAC in the remaining months of FY11.
- The prototype of a fully coupled THMC simulator, TOUGHREACT-FLAC 3D, will be developed in the "Repository Science-THCM Near Field" work package. That development will be used in the EBS work activities in FY12.
- The double-structure model provides the link for incorporating the effects of chemical variables on the mechanical behavior of expansive clays. The linkage and its effects on THMC processes will be investigated.
- The BBM and double-structure capability development will be applied to conduct modeling of DECOVALEX cases, or of a major Mont Terri field experiment.

Reactive-Diffusive Transport

- Improvement of the mean electrostatic potential calculation based on the Donnan equilibrium, so that it captures the observed effective diffusivity over a wider range of conditions (bentonite compaction and ionic strength).
- Calculation of the full Poisson-Boltzmann equation in the vicinity of the charged clay surfaces. This will likely be a nanometer scale version of the approach described above, with a focus on one or at most several clay grains, and will be used to provide guidance on possible approaches for treating the full continuum scale problem.

- Investigation of pore-network-scale modeling for modeling transport through clays.
- Collaboration with Dr. James Davis on a new set of radionuclide tracer experiments through clay (to be funded in part by the "Repository Science-THCM Near Field" work package).

5. Recommended Areas of International Collaboration

5.1 Opportunities and considerations

For the UFD Campaign (UFDC), international collaboration is a beneficial and cost-effective strategy for advancing disposal science in multiple disposal options and different geologic environments. While the United States disposal program had focused solely on Yucca Mountain tuff as host rock, several international programs have made significant progress over the past decades in the characterization and performance evaluation of other geologic repository options, most of which very different from the Yucca Mountain site in design and host rock characteristics. Because Yucca Mountain was so unique (e.g., no backfill, unsaturated densely fractured tuff), areas of direct collaboration with international disposal programs were quite limited during that time. The decision by the U.S. Department of Energy to no longer pursue the disposal of UNF at Yucca Mountain has shifted UFDC's interest to disposal options and geologic environments more in line with many international disposal programs; much can be learned in close collaboration with these programs to get access to valuable experience and data gained over decades. LBNL researchers are actively pursuing opportunities for such collaboration. Jens Birkholzer from LBNL has recently assumed the role of UFDC's Technical Lead for International Activities, and as such, will advise the campaign on international activities with potential for significant technical advances. He will also interact with international organizations and programs to help advance specific collaborations, in particular those that would provide *active* collaboration of UFDC researchers within international R&D projects.

International geologic disposal programs are at different maturation states, ranging from essentially "no progress" to selected sites and pending license applications to regulators. The table below summarizes the status of UNF and HLW management programs in several countries. The opportunity certainly exists to collaborate at different levels ranging from providing expertise to those countries "behind" the U.S. to obtaining access to information and expertise from those countries with mature programs (*Used Fuel Disposition Campaign International Activities Implementation Plan, FCR&D-USED-2011-000016 REV 0, November 2010 [Nutt, 2011]*).

Table 5-1. Summary of UNF and HLW Management Programs in Other Countries

Country	Material to be Disposed	Centralized Storage	Geologic Environments	URL	Site-Selection	Anticipated Start of Repository Operations
Finland	SNF		Granite, Gneiss, Grandiorite, Migmatite	ONKALO (Granite)	Site at Olkiluoto Selected	2020
Sweden	SNF	CLAB - Oskarshamn	Granite	Aspo (Granite)	Site at Osthammar Selected	2023
France	HLW and ILW		Argillite and Granite	Bure (Argillite)	Site near Bure Selected	2025
Belgium	HLW		Clay/Shale	Mol (clay)	Not Initiated	~2040
China	HLW		Granite		Preliminary Investigations Underway - Beishan in Gobi Desert	~2050
Switzerland	HLW	Wulenlingen (ZWILAG)	Clay and Granite	Mont Terri (Clay) Grimsel (Clay)	Initiated	No sooner than 2040
Japan	HLW		Granite and Sedimentary	Mizunami (Granite) Hornonobe (Sedimentary)	Initiated	No Decision Made
Canada	SNF		Granite and Sedimentary	Pinawa (Granite) - being decommissioned	Initiated	No Decision Made
United Kingdom	HLW and ILW		Undecided		Initiated	No Decision Made
Germany	HLW, SNF, heat generating ILW	Gorleben and Ahaus	Salt	Gorleben (Salt)	On Hold	No Decision Made
Republic of Korea	SNF	Envisioned	Granite	Korea Underground Research Tunnel (Granite, Shallow)	Not Initiated	No Decision Made
Spain	No Decision Made	Siting Process Initiated	Granite, Clay, Salt		Not Initiated	No Decision Made

Source: Nuclear Waste Technical Review Board, 2009. Survey of National Programs for Managing High-Level Radioactive Waste and Spent Nuclear Fuel

As to the possible types of international involvement, one may distinguish between two broad categories. The first category comprises participation in multi-national or bilateral organizations, working groups, or committees, and typically involves high-level information exchanges, expert panels, review functions, training and education, etc. Recent or ongoing UFDC (or NE-53) activities in this area have been summarized in *Used Fuel Disposition Campaign International Activities Implementation Plan (FCR&D-USED-2011-000016 REV 0, November 2010 [Nutt, 2011]*). A few selected examples include multi-national activities such as under IAEA (e.g., review activities, conference participation, education within the International training Center, ITC, …), OECD/NEA (e.g., participation in annual meetings, Integration Group for the Safety Case membership, R&D on NEA Thermodynamic Database,…), EDRAM (International Association for Environmentally Safe Disposal of Radioactive Waste), or bilateral agreements such as PUNT (U.S. – China Peaceful Uses of Nuclear Energy) and NEAP (U.S. – Japan Nuclear Energy Action Plan. UFDC will continue participation and/or support of many of the international activities discussed above, and may need to expand on certain activities, but will need to be selective in its choices to further those opportunities that are of most benefit to the campaign.

The second category involves *active* R&D collaboration of UFDC researchers within international projects or programs in close collaboration with multi-national scientists. With active R&D, we mean here that UFDC scientists work together closely with international scientists on concrete research projects relevant to both sides. Such active collaboration would provide direct access to information, data, and expertise on various disposal options and geologic environments that has been collected over the past decades. Many international programs have operating Underground Research Laboratories (URLs) in clay/shale, granite, and salt environments, in which relevant field experiments have been and are being conducted. Depending on the type of collaboration, UFDC researchers

may be able to participate in planning, conducting, and interpreting these experiments, and thereby get early access to field studies without having *in situ* research facilities in the U.S. We consider such active R&D activities to be most beneficial to UFDC, to help efficiently achieve its long-term goals of conducting "experiments to fill data needs and confirm advanced modeling approaches" (by 2015) and of having a "robust modeling and experimental basis for evaluation of multiple disposal system options" (by 2020). Most of LBNL's effort to date was to explore opportunities of active international collaboration, both at our institution and within the UFDC as a whole. Advancing such opportunities will be the primary focus of UFDC's international activities in the next few years. (Obviously, the first category of international involvement discussed above is important in helping identify and facilitate avenues of active R&D collaboration; it is thus important that UFDC or NE-53 continue participation in multi-national or bilateral organizations such as IAEA, or OECD/NEA.)

Active collaboration can be achieved under different working models. One first straight-forward option is informal peer-to-peer interaction with international R&D organizations. Several UFDC scientists, most of which are associated with DOE's national laboratories, have close relationships with their international counterparts, resulting from workshops and symposia meetings, or from active R&D collaboration outside of UFDC's scope. Continued UFDC support for participation of UFDC researchers in relevant international meetings will help to foster and expand such relationships.

Other working models for active collaboration may require formal agreement and sometimes long-term (financial) commitment before R&D collaboration can take place. It is advisable that such agreements with international organizations/partners should be exercised by DOE, rather than by the UFDC or individual DOE national laboratories. Examples of valuable multi-national and multi-partner initiatives that promote active R&D in nuclear waste disposal science and that require DOE "membership" are the DECOVALEX Project, the Mont Terri Project and the Colloid Formation and Migration Project, all of which are further discussed below. Instead of multi-partner initiatives, there may also be direct participation of DOE national laboratories in specific projects run by individual international disposal programs. The latter may or may not require formal bilateral agreements.

The following sections describe in more detail opportunities for active research with international disposal programs. The focus here is on such opportunities that provide access to field data (and respective interpretation/modeling) or may even allow participation in ongoing field experiments. Of these opportunities, we describe in this report near-term options related to the engineered barrier system (EBS) work package of the UFDC, with focus on buffer/backfill and seal behavior, and on the interaction of these materials with other EBS components and the surrounding host rock. (It should be noted, however, that the opportunities discussed here and the recommendations made are also be applicable to other related work packages, in particular to the natural barrier system (NBS), as most of the field experiments include both the EBS and the NBS.) Open R&D issues with respect to EBS have been discussed in previous progress reports (e.g., Steefel et al., 2010), and have been evaluated in consideration of their importance to the safety

case in a recently conducted roadmap exercise (*Used Fuel Disposition Campaign Disposal Research and Development Roadmap, FCRD-USED-2011-000065 Rev 0, March 2011; Tables 7 and 8; [Nutt, 2011]*). Much more detail on any of the below mentioned experimental efforts and initiatives can be provided upon request; point of contact is Jens Birkholzer at Lawrence Berkeley National Laboratory, UFDC's Technical Lead for International Activities.

5.2 DECOVALEX Project

The DECOVALEX Project is a unique international research collaboration, initiated in 1992, for advancing the understanding and mathematical modeling of coupled thermo-hydro-mechanical (THM) and thermo-hydro-mechanical-chemical (THMC) processes in geological systems—subjects of importance for performance assessment of radioactive waste repositories in geological formations. DECOVALEX is an acronym for "Development of Coupled Models and their Validation against Experiments". Starting in 1992, the project has made important progress and played a key role in the development of numerical modeling of coupled processes in fractured rocks and buffer/backfill materials. The project has been conducted by research teams supported by a large number of radioactive-waste-management organizations and regulatory authorities, including those of Canada, China, Finland, France, Japan, Germany, Spain, Sweden, UK, South Korea, Czech Republic, and the USA. Through this project, in-depth knowledge has been gained of coupled THM and THMC processes associated with nuclear waste repositories, as well as numerical simulation models for their quantitative analysis. The knowledge accumulated from this project, in the form of a large number of research reports and international journal and conference papers in the open literature, has been applied effectively in the implementation and review of national radioactive-waste-management programs in the participating countries. A good overview of the project is given in Tsang et al. (2009).

The DECOVALEX Project is typically conducted in separate 3-4 year project phases. Each phase features a small number (typically three to five) modeling test cases of importance to radioactive waste disposal. Many test cases are laboratory and field experiments that have been conducted by one of the project partners and are then collectively studied and modeled by DECOVALEX participants. Numerical modeling of these test cases can assist both to interpret the test results and to test the models used. Over the years, a number of large-scale, multiyear field experiments have been studied within the project (e.g. the Kamaishi THM Experiment, FEBEX, and the Yucca Mountain drift scale heater test). Thus the project provides access to valuable technical data and expertise to DECOVALEX partner organizations; this is particularly useful in disposal programs that are starting their research on certain disposal or repository environments and have no URLs. DECOVALEX has a modeling focus, but tight connection to experimental data.

In order to participate in a given DECOVALEX phase, interested parties—such as waste management organizations or regulatory authorities—need to formally join the project and pay a small annual fee that covers administrative and technical matters. In addition to

this fee, participating organizations provide funding to their own research teams to work on some or all of the problems defined in the project phase. Representatives from the funding organizations form a Steering Committee that collectively directs all project activities.

DOE was a DECOVALEX partner for several project phases, but decided to drop out in 2007 with the increasing focus on the license application for Yucca Mountain. Now that the U.S. has shifted to other disposal options and geologic environments, a renewed engagement of DOE with DECOVALEX would provide UFDC researchers access to relevant field data from international programs and allow them to work collaboratively with international scientists on analyzing and modeling these data. The next DECOVALEX phase, referred to as DECOVALEX-2015, will start in early 2012. A planning session for this next DECOVALEX phase was held in a recent workshop in Helsinki, and several modeling test cases involving field data were proposed by prospective funding organizations.

- HE-E Heater Test: Studies of bentonite/rock interaction to evaluate sealing and clay barrier performance, in a micro-tunnel at the Mont Terri URL, proposed by ENRESA (Spain)
- SEALEX Experiment: A long term test of the hydraulic (sealing) performance of a swelling bentonite core (5 m long) in a mini tunnel (60 cm diameter) at the Tournemire URL in France, proposed by ISRN (France)
- MB Test: Mine-by test studying pore pressure and stress evolution during excavation, at the Mont Terri URL, proposed by NAGRA (Switzerland)
- Bedrichov Tunnel Experiment: Interpretation of inflow patterns and tracer transport behavior in a fractured granite, proposed by NAWRA (Czech Republic)
- THMC Processes in Single Fractures: Modeling of laboratory experiments on mechano-chemical impacts on fracture flow, tentatively proposed by KAERI/LBNL (South Korea/USA)
- Possible revisits of past DECOVALEX phases for the purpose of identifying potential tasks containing unsolved but important issues, tentatively proposed by CEA (France)

Of the five experimental data sets, the first two are highly relevant to the EBS work package of UFDC, as both target the behavior of backfill and sealing materials in interaction with clay host rock. More details on these two experiments, the HE-E Heater Test and the SEALEX Experiment, are given below. (The other proposed test cases are more relevant to the NBS work package of UFDC.) The DECOVALEX secretariat will soon distribute short summaries of each suggested test case.

One issue to resolve soon is the question as to how to handle the cost of international commitments such as the DECOVALEX project. A possible solution is that the "membership fee" for DOE participation would come out of some centralized international fund, while the staff support for active R&D would be covered out of the relevant UFDC work packages (e.g., EBS, NBS). The expected “membership fee” for DECOVALEX 2015 is about $42,000, somewhat dependent on the final number of

participating organizations as well as the currency exchange rate. In the case of the DECOVALEX project, DOE membership ensures that any national laboratory associated with DOE would be allowed to participate.

HE-E Heater Test at Mont Terri URL, Switzerland

The HE-E Heater Test at the Mont Terri URL, shown in Figure 5.1, focuses on the THM behavior of bentonite barriers in the early non-isothermal resaturation stage and their THM interaction with Opalinus Clay (see Section 5.3 for more information on the Mont Terri URL). The objective is to better understand the evolution of a disposal system of high level waste in the early post-closure period with emphasis on the thermal evolution, buffer resaturation (in situ determination of the thermal conductivity of bentonite and its dependency on saturation), pore water pressure in the near field, and the evolution of swelling pressures in the buffer. Because the test is conducted in a micro-tunnel (at 1:2 scale), it is considered a validation, not a demonstration experiment. The heating test involves two types of bentonite buffer materials. The heater-buffer interface will be heated to a maximum of 135°C and a temperature of 60-70°C is expected at the buffer-rock interface. A dense instrumentation network is already in place in the host rock surrounding the micro-tunnel (from a previous experiment testing the impact of ventilation on the clay host rock) and will be improved (up to 40 piezometers in total); various sensors will also be placed in the buffer material. Heating is expected to start in late summer of 2011 and will be continued for at least three years.

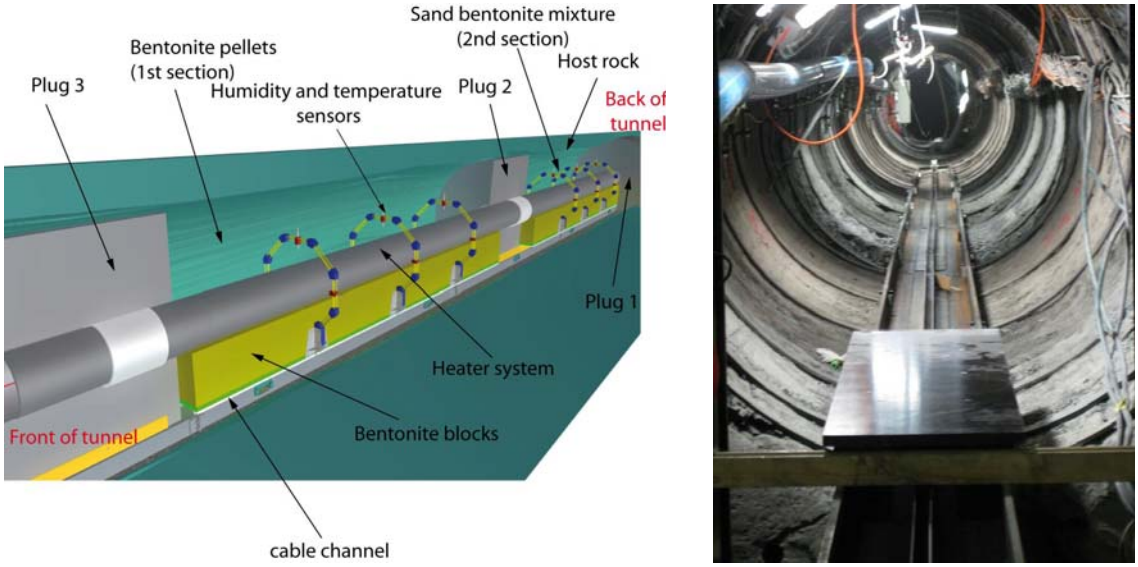

Figure 5.1. Schematic setup of HE-E heater test at Mont Terri and photo of micro-tunnel (from Garitte et al, 2011)

SEALEX Experiment at the Tournemire URL,France

The SEALEX experiment aims at investigating the long-term HM behavior and hydraulic performance of swelling clay-based seals (Figure 5.2). A suite of experiments will be

conducted in several 60-cm diameter mini-tunnels (5 m long) that are exposed to nominal conditions, different technological choices for seal mixtures and emplacement, and altered situations (e.g., forced resaturation or not; loss of mechanical confinement or not) (Figure 5.3). Forced resaturation can lead to heterogeneous saturation and porosity/permeability fields within the bentonite core, and hence the possibility of clay-core erosion due to flow channeling. The experiments will test these hydraulic parameters and their spatial distribution via state-of-the-art measurement technology (e.g., wireless sensors installed within the core to limit preferential flow along cables). Hydraulic tests (pulse tests + constant load tests) will eventually be conducted to determine the overall hydraulic properties (permeability, leaks) of the seals, for different representative conditions. While not decided yet, IRSN considers adding one particular test to the experimental plan that would evaluate HMC behavior with concrete/steel and concrete/bentonite interaction.

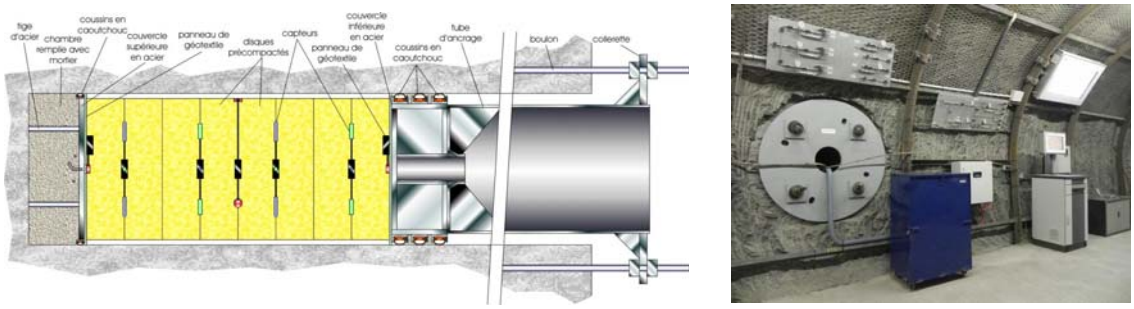

Figure 5.2. Schematic setup of mini-tunnel with seal core and instrumentation (left); view from gallery after core emplacement (right) (from Barnichon, 2011)

	Reference Tests	Performance Tests	Intra-core geometry Core conditioning Composition (MX80/sand)	Core view	Altered conditions	Emplacement date
Base case	RT-1	PT-N1	Monolithic disks Precompacted (70/30)		No	12/2010 06/2011
Variations / Base case	-	PT-A1	Monolithic disks Precompacted (70/30)		Confinement loss	06/2012
	-	PT-N2	Disks + internal joints (4/4) Precompacted (70/30)		No	12/2011
	RT-2	PT-N3	Pellets/powder In situ compacted (100/0)		No	12/2012 06/2013
	-	PT-N4	Monolithic disks Precompacted (20/80)		No	12/2013

Figure 5.3. Planned experiments and schedule (from Barnichon, 2011)

The SEALEX experiments are conducted at the Tournemire URL in the south of France. This site is characterized by a sub-horizontal indurated argillaceous claystone layer 250 m thick. A railway tunnel, constructed in 1881 through the argillaceous formation, is 2 km long, 6 m high and 4.7 m wide, and was excavated using a pneumatic tool. In 1996 and 2003, additional research tunnels were excavated off the main railway tunnel. Thus, this facility allows study of near field rock behavior in indurated clay with different time periods of exposure to the atmosphere, namely 130, 15 and 8 years, respectively (Rejeb and Cabrera, 2006) (Figure 5.4).

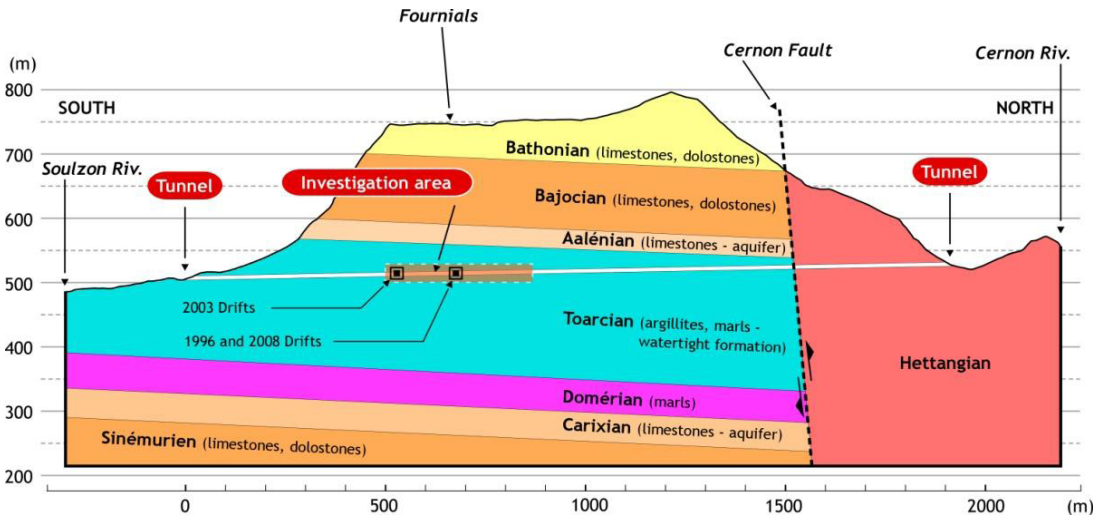

Figure 5.4. Geological cross-section of the Tournemire site, South France (from Rejeb and Cabrera, 2006) (from Barnichon, 2011)

5.3 Mont Terri Project

The Mont Terri Project is an international research project for the hydrogeological, geo-chemical and geotechnical characterisation of a clay/shale Formation suitable for geologic disposal of radioactive waste (Zuidema, 2007). The project utilizes an underground rock laboratory, which lies north of the town of St-Ursanne in Northeastern Switzerland and is located at a depth of around 300 meters below the surface in argillaceous claystone (Opalinus Clay). Construction of the facility in conjunction with a motorway tunnel started in 1987, and the Mont Terri Project was officially initiated in 1996 (Figure 5.5). (http://www.mont-terri.ch/ids/default.asp?TopicID=72).

Often using co-sponsorship from European Community funds, the project essentially operates as a collaborative program providing open access to an existing URL. Mont Terri partner organizations may select and conduct experiments, and they have access to all project results from past and ongoing efforts. Larger field experiments are often conducted by more than one organization. Current project partners are from Switzerland (swisstopo/SGS, ENSI, NAGRA), Belgium (SCK/CEN), France (ANDRA, IRSN),

Germany (BGR, GRS), Japan (OBAYASHI, JAEA, CRIEPI), Spain (ENRESA, Empresa), Canada (NWMO), and USA (CHEVRON).

Participation of DOE as a partner in the Mont Terri Project would provide UFDC researchers access to relevant field data and project results from past efforts. Mont Terri has been in operation for a long time, and a wide range of experimental studies on clay/shale behavior (including backfill/buffer behavior) have already been conducted. More importantly, UFDC researchers could work collaboratively with international scientists on *ongoing and future* experimental studies, which would include all design, characterization, modeling, and interpretation aspects related to field experiments and. In the long term, UFDC researchers would also be able to propose and eventually conduct their own experiments at the Mont Terri URL. This type of international collaboration goes beyond the mostly modeling focus of DECOVALEX, and may arguably be the most fruitful approach to active international R&D. Three prominent experiments are currently being conducted or are in preparation stages, two of which are also proposed as DECOVALEX modeling test cases (e.g., the HE-E Heater Test and the MB Mine-By Test). The third one, referred to as FE Heater Test (described below in more detail), is a long-term (> 10 years), full-scale test that will serve as an ultimate validation and demonstration test for emplacement of heat-producing waste in Opalinus Clay, at realistic temporal and spatial scales. Validation will include THM coupling effects with focus on both the EBS components and the host rock behavior.

In order for DOE to become a formal Mont Terri partner, there are two main rules: (1) The present Mont Terri Project partners have to unanimously accept new partner organizations, and (2) As a buy-in, new partners have to invest an amount of about 500K Swiss Francs (about $500K), which can be spread over a period of 3 years. The buy-in fee can partially be provided in kind (i.e., by having UFDC researchers conduct work). The fraction of in-kind contributions can be negotiated with the Mont Terri partners, but is expected to be somewhere between 30 to 50% of the total. In addition to the "membership fee" for DOE participation, staff support for active R&D would have to be covered out of the relevant UFDC work packages (e.g., EBS, NBS).

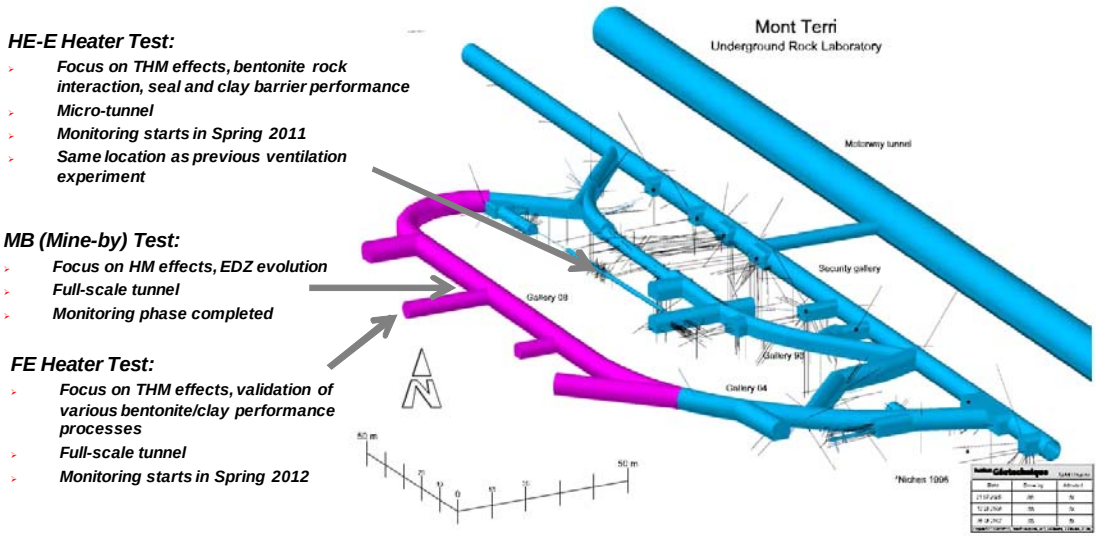

Figure 5.5. Summary schematic of the Mont Terri URL with side galleries and drifts for testing (based on Garitte, 2010)

Because of its potential relevance to UFDC's EBS and NBS areas, we provide here some further detail on the FE Heater Test, one of the largest and longest-duration heater tests worldwide. As mentioned before, this heater experiment is undertaken by NAGRA and other European partners as an ultimate test for the performance of geologic disposal in Opalinus Clay, with focus on both the EBS components and the host rock behavior. The experiment will provide data useful for the validation of THM coupling effects regarding the processes in the host rock while correctly accounting for (and examining) the conditions in the emplacement tunnel (temperature, saturation, and swelling pressure). Due to the 1:1 scale of the experiment, it will be possible to achieve realistic temperature, saturation, and stress gradients. It will also be possible to test backfilling technology with granular bentonite as well as lining technology with shotcrete, anchors and steel rips. Processes examined in the test cover many aspects of repository evolution, such as EDZ creation and desaturation of the EDZ during tunnel excavation and operation (including ventilation for about one year), as well as reconsolidation of the EDZ, resaturation, thermal effects, thermal stresses, and thermal pore pressure increase after backfilling and heating (heating and monitoring period > 10 years).

As shown in Figure 5.6, the FE Heater Test will be conducted in a side tunnel at Mont Terri, excavated along the claystone bedding plane for this purpose, with 50 m length and about 2.8 m diameter. Heating from emplaced waste will be simulated by three heat-producing canisters of 1500 W maximum power. A sophisticated monitoring program is planned, including dense pre-instrumentation of the site for in-situ characterization, dense instrumentation of bentonite buffer and host rock, and extensive geophysical monitoring (seismic and electric "tomography"). A THM modeling program will be conducted in parallel with the testing and monitoring activities.

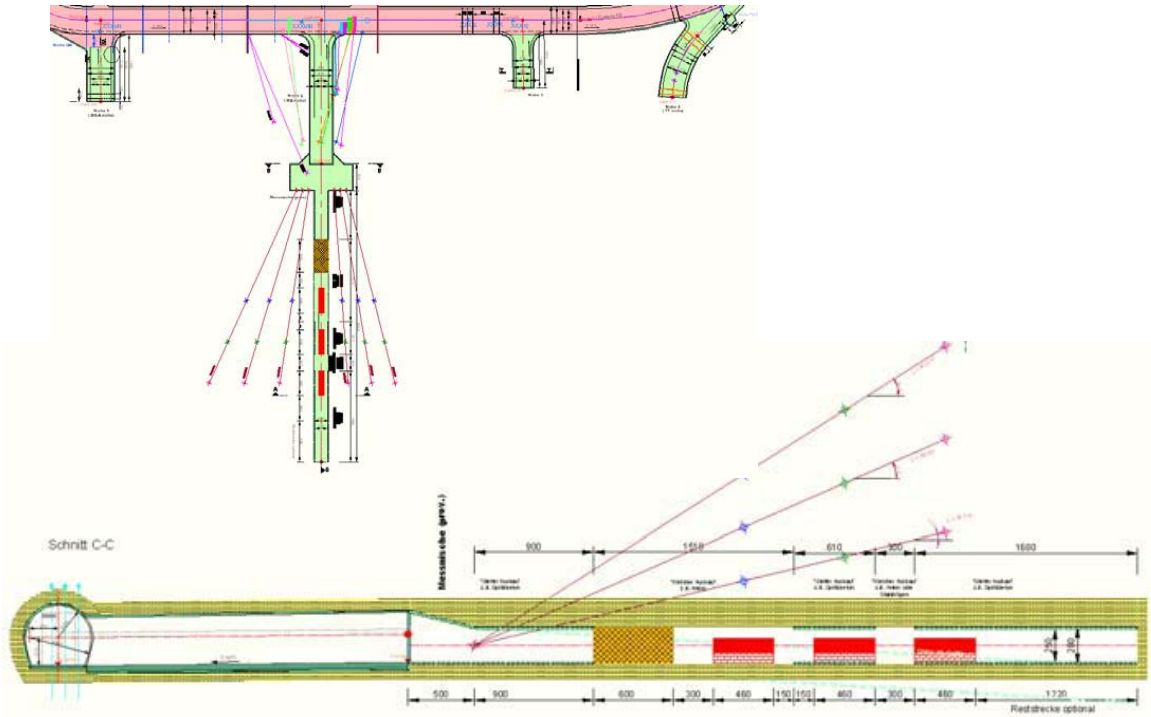

Figure 5.6. Plan (top) and side view (bottom) of experiment setup and observation borehole layout (from Garitte, 2010)

5.4 Colloid Formation and Migration (CFM) Project

The Colloid Formation and Migration Project is an international research project for the investigation of colloid formation/bentonite erosion, colloid migration, and colloid-associated radionuclide transport, relevant to both EBS and NBS areas of UFDC. This collaborative project is associated with the Grimsel Test Site (GTS) in the Swiss Alps, a URL situated in sparsely fractured crystalline host rock (http://www.grimsel.com/). Colloid-related R&D comprises *in situ* field work, but also laboratory and modeling studies. Current project partners are from Germany (BMWi), Japan (JAEA, CRIEPI), Sweden (SKB), South Korea (KAERI), Finland (POSIVA), and Switzerland (NAGRA). The main R&D objectives, relevant to both EBS and NBS issues, are as follows:

- To examine colloid generation rates and mechanisms at the Engineered Barrier System (EBS) - host rock boundary under in situ conditions,
- To evaluate the long-distance migration behavior of EBS-derived colloids in a water-conducting feature in a repository relevant flow system (i.e. with a very low flow rate/water flux),
- To study the long-term geochemical behavior (mobility, mineralization, colloid formation, etc) of radionuclides at the EBS-host rock boundary,
- To examine reversibility of radionuclide uptake onto colloids,

- To gain experience in long-term monitoring of radionuclide/colloid propagation near a repository

A series of colloid-facilitated radionuclide field transport experiments have been conducted at the Grimsel Test Site, and more of these CFM field tests are planned for future years. With respect to EBS-related issues, a new field experiment is planned to start in late 2011; it will involve the emplacement of a radionuclide-doped bentonite plug into a Grimsel borehole followed by long-term monitoring (over many years) for both colloids and radionuclides (Figure 5.7). The bentonite emplacement borehole supplies the access for the colloid source to a water conducting feature in the crystalline host rock, outside the influence of the GTS tunnel system. The formation and transport of colloids and colloid-associated radionuclides is then monitored utilizing an array of down-gradient boreholes drilled at various travel distances into the shear zone. In order to evaluate the transport under near-natural flow conditions, the shear zone is hydraulically isolated by installing a sophisticated mega-packer system, counteracting the natural gradient towards the tunnel surface.

Similar to the Mont Terri Project discussed above, DOE may consider becoming a formal partner of the Colloid Formation and Migration Project (CFM). Formal partnership would give DOE and affiliated national laboratories access to CFM data from past and ongoing experiments, would allow for UFDC researchers to work collaboratively with international scientists on *ongoing* experimental studies, and would involve them in the planning of new experimental studies to be conducted in the future. DOE partnership would require a “membership contribution” of approximately $95K per year based on the current participation level of 85K Swiss Francs per year by the other partners. It is likely that a commitment of at least three years is required, but this has yet to be confirmed. In addition to the "membership fee" for DOE participation, staff support for active R&D would have to be covered out of the relevant UFDC work packages (e.g., EBS, NBS).

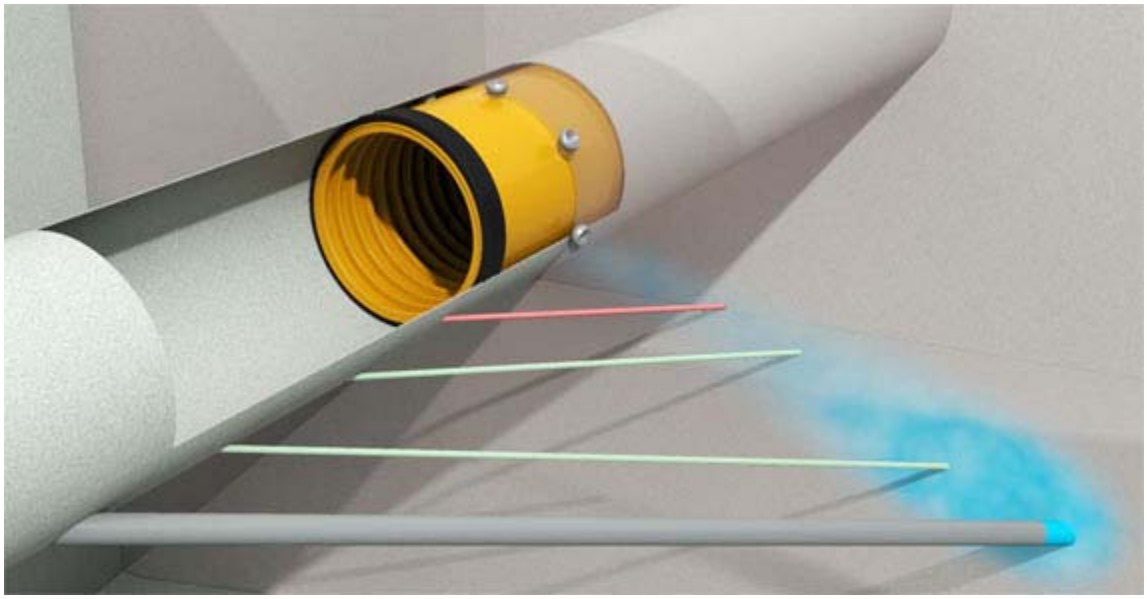

Figure 5.7. Schematic setup of bentonite plug and colloid transport experiment (from http://www.grimsel.com/gts-phase-vi/cfm-section/cfm-concept)

5.5 Other active collaboration opportunities

In some cases, access to data on international field experiments and participation of UFDC researchers in collaborative field studies may also be facilitated via informal or semi-formal agreements directly between national laboratories and international partners. Several UFDC scientists already have close relationships with their international counterparts, resulting from workshops and symposia meetings, or from collaboration outside of UFDC's scope. International disposal programs are aware of the technical capabilities of UFDC scientists and are generally quite open to include them in their ongoing research teams. This may or may not require bilateral MoUs or other types of agreements.

Below is a short list of major (soon-to-start or planned) field experiments conducted by international disposal programs that may be open to national laboratory participation, without "membership fees" or other long-term commitments on behalf of DOE.

PRACLAY Test at HADES URL in Belgium:

The PRACLAY Heater Test is a full-scale validation and confirmation experiment to be conducted at the HADES (High Activity Disposal Experimental Site) URL, excavated at 223 m depth in Boom Clay, a tertiary clay formation in Mol, Belgium. The heater test, which will begin in late 2011 or early 2012, will involve heating a 30 m gallery section for 10 years with many monitoring sensors, for the purpose of investigating the thermo-hydro-mechanical (THM) behavior of plastic clay under the most "penalizing" conditions that may occur around a repository (Van Marcke and Bastiaens, 2010) (Figure 5.8). These include THM behavior of plastic clay under undrained conditions. For this

objective, a hydraulic seal will be installed at the intersection between the planned heated and unheated sections of the gallery. This installation makes up the Seal Test, which was initiated in 2010, and allows testing the functionality of the hydraulic seal under heated repository conditions. The Belgium organizations involved in conducting and interpreting these experiments (EIG Euridice, SCK CEN, ONDRAF/NIRAS) have long-standing relationships to scientists at Lawrence Berkeley National Laboratory (LBNL); they have already invited LBNL researchers to provide THM modeling expertise to the project team.

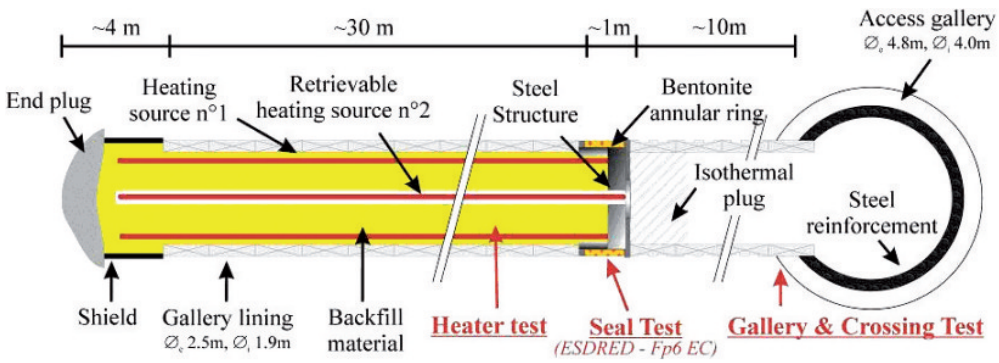

Figure 5.8. Layout of the PRACLAY In-Situ Experiment which is constituted of the the Seal Test, and the actual Heater Test (from Van Marcke and Bastiaens, 2010)

Gas-Permeable Seal Test (GAST) at Grimsel Test Site, Switzerland

The objective of the soon-to-start GAST experiments is to demonstrate the construction and performance of repository seals and plugs and to improve the understanding and the base datasets for reliably predicting water and gas transport through these sealing systems. The experiment will test a specific design option called "engineered gas transport system (EGTS)" (Figure 5.9), which involves specially designed backfill and sealing materials such as high porosity mortars or sand/bentonite (S/B) mixtures. The reason to develop these special designs is to allow for increased gas transport capacity (to mitigate pressure buildup from gas generation) of the backfilled underground structures without compromising the radionuclide retention capacity of the engineered barrier system. The managing organization for this experiment is NAGRA (Switzerland); a few other European partners are also involved. NAGRA has expressed that it would possibly be open for UFDC scientists to participate in aspects of the experiment.

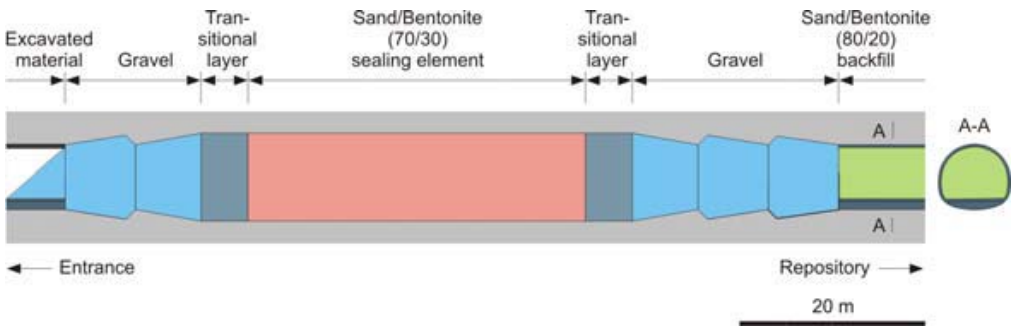

Figure 5.9. Schematic picture of repository seal design for GAST experiment (from Vomvoris, 2011)

Large-Scale Gas Injection Test (LASGIT) at Äspö URL, Sweden

This ongoing field experiment, which has been in operation for over five years, evaluates gas flow processes (related to the potential for gas generation from canister corrosion) in an unsaturated bentonite embedded in fractured crystalline rock. Current knowledge pertaining to gas flow in a compact saturated bentonite is based on small-scale laboratory studies; the LASGIT tests are designed to address specific issues relating to gas migration and its long-term effect on the hydro-mechanical performance of the buffer clay, the question of heterogeneity and tortuosity of flow paths and the possible generation of new flow paths, and the complex coupling between gas, stress, and porewater pressure at different scales. The main organization conducting the experiment is SKB (Sweden), together with the British Geological Survey (BGS). The GASIT experiment was initially proposed as a modeling test case for DECOVALEX-2015, but is not under consideration anymore. However, SKB and BGS may be open to collaboration or participation of UFDC scientists.

Figure 5.10. GASIT experiment at Äspö (from Cuss, 2010)

Bentonite Rock Interaction Experiment (BRIE) at Äspö URL, Sweden

Another option for UFDC engagement may be the upcoming BRIE test to be conducted at the Äspö URL in Sweden. The main objective of this experiment is to enhance the understanding of the hydraulic interaction between the fractured crystalline rock at Äspö and unsaturated bentonite. The setup is aligned with the Swedish concept of emplacing canisters into vertical deposition holes that are subsequently backfilled. The main organization conducting the experiment is SKB (Sweden).

Other Participation Options for Mont Terri Project and CFM Experiments

Note that some benefits that the above-mentioned multi-national and multi-partner initiatives (such as the Mont Terri Project or the Colloid Formation and Migration Project) can provide to UFDC may also be achievable via less formal partnerships. For example, LBNL has been offered the opportunity to become one of NAGRA's modeling and analysis partners for the full-scale FE Heater experiment at Mont Terri. Similarly, scientists at Los Alamos National Laboratory (LANL) have been engaged in the Colloid Formation and Migration Project without DOE being a full partner, and could presumably continue to do so. However, in both cases, without formal agreement, LBNL's and LANL's role would be limited to ad-hoc contributors. Full partnership, on the other hand, would give *all* DOE national laboratories full access to *all* of the many experiments that have been or will be conducted within the Mont Terri Project and CFM, respectively. Full partnership would also allow for DOE to be in a position to propose or conduct its own suite of experiments.

5.6 Recommendations and path forward

Active collaboration with international programs, initiatives, or projects is considered very beneficial to UFDC, providing access to the decades of experience that some international programs have in various disposal options and geologic environments. We postulate that increasing international engagement will help efficiently achieve UFDC's long-term goals of conducting "experiments to fill data needs and confirm advanced modeling approaches" (by 2015) and of having a "robust modeling and experimental basis for evaluation of multiple disposal system options" (by 2020). Above report section discusses different opportunities of active international collaboration, with focus on EBS aspects and those opportunities that provide access to field data (and respective interpretation/modeling) or allow participation in ongoing field experiments. Similar assessments are ongoing with focus on NBS aspects, and will be documented in an upcoming NBS status report.

The next step will be to develop a concise list of promising international opportunities, which documents their cost and benefits, the mode of participation, and the key research gaps addressed (with tight link to roadmap and FEPs importance ranking; using the *Used Fuel Disposition Campaign Disposal Research and Development Roadmap, FCRD-USED-2011-000065 Rev 0, March 2011 [Nutt, 2011]*). Based on this, potential activities will be ranked and recommendations will be made in time for the DOE/NE-53 and UFD planning process for FY12 and beyond. An early decision point is about DOE's possible

participation in international agreements such as the DECOVALEX Project, the Mont Terri Project, and the Colloid Formations and Migration Project.

6. Summary

Bentonite and bentonite-sand mixtures have been found to have favorable properties for use as a backfill/buffer material for nuclear waste repositories. This report focuses on analyses of bentonite as a component of the EBS. Specific analyses presented here highlight progress made in areas of THM coupled processes models and reactive transport models for bentonite. These research activities address key Features, Events and Processes (FEPs) with rankings from medium to high listed in Tables 7 and 8 of *Used Fuel Disposition Campaign Disposal Research and Development Roadmap* (FCR&D-USED-2011-000065 REV0) (Nutt, 2011).

THM Process Modeling in Bentonite

In FY10, LBNL incorporated the BBM into the TOUGH-FLAC simulator. The BBM is the most advanced and accepted constitutive model used for modeling of bentonite-buffer behavior in the various European and Japanese nuclear waste programs. In FY11, we have focused so far on using this new capability to model THM processes within EBS and its interactions with natural systems (clay formations) and simulate the sensitivities of a number of processes and interactions to a variety of parameters. It is demonstrated that the maximum temperature and temperature-time behavior of the canisters are determined principally by the canister and areal thermal loading—which are controllable parameters—and the ambient temperature and thermal properties of the bentonite backfill and rock, including buffer saturation and thermal conductivity, tunnel and canister spacing, and rock thermal conductivity. The time to full resaturation of bentonite and swelling depends on a number of parameters, most importantly the hydraulic properties of the rock and the bentonite. For a host rock with the anisotropic strength properties similar to those of Opalinus clay at Mont Terri, our modeling results show that most of the rock mass failure around the tunnel occurs already during the excavation and the development of the swelling pressure in the buffer can prevent further rock failure from occurring.

In what remains of FY11 and in FY12, we will incorporate the dual-structure model into the TOUGH-FLAC simulator to more accurately simulate the THMC processes in the EBS, to develop a fully coupled THMC capability by integrating with research activities in the “Repository Science-THCM Near Field” work package, and to apply the developed capabilities to modeling and analyzing field tests in international sites. The latter can also serve as an important way to verify the model-capability developments.

Reactive-Diffusive Transport in Bentonite

In FY10, we performed a comprehensive literature review of modeling approaches for reactive-diffusive transport in bentonite, with key modeling issues identified and documented in the FY10 final report. In FY11, we have focused on using the newly

developed explicit diffuse double layer capability in CrunchFlow, along with analytical solutions that apply to the binary salt case, to attempt a predictive continuum model for diffusion through compacted bentonite. Also, we have compared our model with the "ion equilibrium" approach of Birgersson and Karnland (2009), based on a single porosity within the clay interlamellae. Our preliminary results show that significant improvements of the currently existing models are needed to accurately reproduce experimental observations.

In the remaining months of FY11 and in FY12, we will continue to refine our predictive continuum model for diffusion by improving the mean electrostatic potential calculation based on the Donnan equilibrium, develop approaches to calculating the full Poisson-Boltzmann equation in the vicinity of the charged clay surfaces, model transport through clays with pore-network-scale models, and collaborate with Dr. James Davis at LBNL on a new set of radionuclide tracer experiment through clay (planned as part of the "Repository Science-THCM Near Field" work package).

International Collaborations

Active collaboration with international programs, initiatives, or projects is very beneficial to UFDC, providing access to the decades of experience that some international programs have in various disposal options and geologic environments. This report discusses different opportunities of active international collaboration, with focus on EBS aspects and those opportunities that provide access to field data (and respective interpretation/modeling) or allow participation in ongoing field experiments. Similar assessments are ongoing with focus on NBS aspects, and will be documented in an upcoming NBS status report.

As the next step, Jens Birkholzer will develop a concise list of promising international opportunities, which documents their cost and benefits, the mode of participation, and the key research gaps addressed. Based on this, potential activities will be ranked and recommendations will be made in time for the DOE/NE-53 and UFD planning process for FY12 and beyond.

Integration with Other Work Packages

Research and development activities in the EBS work package have been closely integrated with related activities in other work packages in which LBNL has been involved. For example, a protocol of fully coupled THMC simulators (TOUGHREACT-FLAC3D) is currently under development in the "Repository Science-THCM Near Field" work package. The BBM evaluated and used in this study will be incorporated into the TOUGHREACT-FLAC3D simulator. This simulator is expected to provide modeling capabilities for THMC processes in the EBS. Constitutive relationships that are under development in the natural system will be employed for studying interactions between natural systems (clay formations) with EBS. An experimental study of chemical diffusion in clay materials is planned as part of the "Repository Science-THCM Near Field" work package(Jim Davis). Observations from those laboratory experiments will be used to further develop our predictive continuum model for diffusion through compacted

bentonite. Furthermore, the development of the diffusion model has provided useful information and guidance for LBNL's research activity related to developing a phenomenological modeling approach for diffusion in clay, in the work packge of Generic Disposal System-Level Modeling.

7. References

Alonso, E.E., J. Vaunat, A. Gens, Modelling the mechanical behaviour of expansive clays. Engineering Geology 54: 173–183, 1999.

Appelo, C.A.J., A . Vinsot, S. Mettler, S. Wechner, Obtaining the porewater composition of a clay rock by modeling the in- and out-diffusion of anions and cations from an in-situ experiment, Journal of Contaminant Hydrology 101: 67–76, 2008.

Birgersson, M., O. Karnland, Ion equilibrium between montmorillonite interlayer space and an external solution - Consequences for diffusional transport, Geochimica et Cosmochimica Acta 73:1908–1923, 2009.

Barnichon, J.D., IRSN proposal - the SEALEX In Situ Tests, Presentation given at 7th DECOVALEX 2011 workshop, April 2011, Helsinki.

Bourg, I.C., A.C.M. Bourg, G. Sposito, Modeling diffusion and adsorption in compacted bentonite: a critical review, J. Contam. Hydrol. **61**, pp. 293–302, 2003.

Bourg, I.C., G. Sposito, A.C.M. Bourg, Tracer diffusion in compacted, water-saturated bentonite, Clays Clay Miner. **54**, pp. 363–374, 2006.

Bourg, I.C., G. Sposito, A.C.M. Bourg, Modeling cation diffusion in compacted water-saturated sodium bentonite at low ionic strength. Environ. Sci. Technol. 41, 8118–8122, 2007.

Corkum A.G., C. D. Martin, Modeling a mine-by test at the Mont Terri rock laboratory, Switzerland. International Journal of Rock Mechanics & Mining Sciences 44: 846-859, 2007.

Cuss, R., Large scale gas injection test (Lasgit): Progress to May 2010, Presentation given at 6th DECOVALEX 2011 workshop, October 2010, Wuhan.

Donat, R., A.Akdogan, E. Erdem, H. Cetisli, Thermodynamics of Pb^{2+} and Ni^{2+} Adsorption onto Natural Bentonite from Aqueous Solutions, Journal of Colloid and Interface Science, Vol. 286, pp. 43-52, 2005.

Garitte, B., and others, HE-E experiment - In situ Heater Test, Presentation given at 7th DECOVALEX 2011 workshop, April 2011, Helsinki.

Garitte, B., New In Situ Experiments at Mt Terri, Presentation given at 6th DECOVALEX 2011 workshop, October 2010, Wuhan.

Gaucher, E.C., P. Blanc, J.M. Matray, N. Michau, Modeling Diffusion of an Alkaline Plume in a Clay Barrier, Applied Geochemistry 19: 1505–1515, 2004.

Gens, A., J. Vaunat, B. Garitte, B., Y.Wileveau, In situ behaviour of a stiff layered clay subject to thermal loading: observations and interpretation. Geotechnique 57, No. 2, 207–228. 2007.

Glaus, M., B. Baeyens, M. Bradbury, A. Jakob, L. Van Loon, A. Yaroshchuk, Diffusion of ^{22}Na and ^{85}Sr in montmorillonite: evidence of interlayer diffusion being the dominant pathway at high compaction, Environmental Science and Technology 41: 478–485, 2007.

Gonçalvès, I., P. Rousseau-Gueutin, A. Revil, Introducing interacting diffuse layers in TLM calculations: a reappraisal of the influence of the pore size on the swelling pressure and the osmotic efficiency of compacted bentonites, J. Colloid Interface Sci. **316,** pp. 92–99, 2007.

Houseworth, J.E., The DOE Used Fuel Disposition Campaign Features, Events, and Processes (FEP) Evaluation Report for Bentonite/Clay/Shale Systems, DOE Used Fuel Disposition Campaign, Lawrence Berkeley National Laboratory. 2010.

Kim, H., T. Suk, S. Park, C. Lee, Diffusivities for ions through compacted Na bentonite with varying dry bulk density, Waste Manag. 13: pp. 303–308, 1993.

Kirby, B., Micro- and nanoscale fluid mechanics, Transport in microfluidic devices, Cambridge University Press, New York, 2010.

Khan, S.A., Sorption of Long-Lived Radionuclides Cesium-134, Strontium-85 and Cobalt-60 on Bentonite, Journal of Radionanalytical and Nuclear Chemistry, Vol. 258, No. 1, pp. 3-6, 2002.

Lemmens, K., The Effect of Clay on the Dissolution of Nuclear Waste Glass", Journal of Nuclear Materials, Vol. 298, pp. 11-18, 2001.

Leroy, P., A. Revil, A triple-layer model of the surface electrochemical properties of clay minerals, Journal of Colloid and Interface Science 270:371–380, 2004.

Leroy, P., A. Revil, D. Coelho, Diffusion of ionic species in bentonite, J. Colloid Interface Sci. 296 (1), pp. 248–255, 2006.

Madsen, F.T., Clay mineralogical investigations related to nuclear waste disposal. Clay Miner. 33, 109-129, 1998.

Muurinen A., Diffusion of anions and cations in compacted sodium bentonite. VTT Publication 168, Espoo Technical Centre, Finland, 1994.

NAGRA, Project opalinus clay. Safety Report. Demonstration of disposal feasibility for spent fuel, vitrified high-level waste and long-lived intermediate-level waste (2002). TR 02-05.

Nutt, M., Used Fuel Disposition Campaign International Activities Implementation Plan, (FCR&D-USED-2011-000016 REV 0), U.S. DOE Used Fuel Disposition Campaign, 2010

Nutt, M., Used Fuel Disposition Campaign Disposal Research and Development Roadmap (FCR&D-USED-2011-000065 REV0), U.S. DOE Used Fuel Disposition Campaign, 2011.

OECD, Engineering barrier systems and the safety of deep geological repositories (State-of-the-art Report), ISBN 92-64-18498-8, 2003.

Ochs, M., B. Lothenbach, H. Wanner, H. Sato, M. Yui, An integrated sorption–diffusion model for the calculation of consistent distribution and diffusion coefficients in compacted bentonite, J. Contam. Hydrol. 47: 283–296, 2001.

Pusch, R. The microstructure of MX-80 clay with respect to its bulk physical propertiunder different environmental conditions. SKB, TR-01-08, 111 p., 2001.

Rejeb, A., J. Cabrera, Time-dependent evolution of the excavation damaged zone in the argillaceous Tournemire Site (France). Proceedings "GeoProc 2006," Invited lecture in the 2nd International Conference on Coupled THMC Processes in Geosystems and Engineering, May 22-25 2006, Nanjing, China, pp. 65-74.

Sabodina, M.N., S.N. Kalmykov, Y.A. Sapozhnikov, E. V. Zakharova, Neptunium, Plutonium, and 137Cs Sorption by Bentonite Clays and their Speciation in Pore Waters, Journal of Radioanalytical and Nuclear Chemistry, Vol. 270, No. 2, pp. 349-355, 2006.

Samper, J., C. Lu, L. Montenegro, Reactive Transport Model of Interactions of Corrosion Products and Bentonite, Physics and Chemistry of the Earth 33: S306–S316, 2008.

Sondi, I., J. Biscan, V. Pravdic, Electrokinetics of pure clay minerals revisited, Journal of Colloid and Interface Science 178 : 514–522C, 1996.

Steefel, C., Development of an explicit diffuse layer model for CrunchFlow, 2010.

Steefel, C., J. Rutqvist, C.F. Tsang, H.H. Liu, E. Sonnenthal, J. Houseworth, J. T. Birkholzer, Reactive Transport and Coupled THM Processes in Engineering Barrier Systems (EBS), Lawrence Berkeley National Laboratory (LBNL), Final Report of FY2010 Activities, Berkeley, August 2010.

Tsang, C.-F., O. Stephansson, L. Jing, L., F. Kautsky, DECOVALEX Project: from 1992 to 2007, Environmental Geology, 57, 1221–1237, 2009

Van Genuchten, M.Th., A closed-form equation for predicting the hydraulic conductivity of unsaturated soils, Soil Sci. Soc. Am. J., 44: 892-898, 1980.

Van Loon, L., M. Glaus, W. Müller, Anion exclusion effects in compacted bentonites: Towards a better understanding of anion diffusion, Applied Geochemistry 22: 2536–2552, 2007.

Van Marcke, P., W. Bastiaens, Construction of the Praclay Experimental Gallery at the Hades URF. Clay in Natural and Engineered Barriers for Radioactive Waste Confinement, 4th International Meeting, March, 2010, Nantes, France.

Vomvoris, S., Personal Communication. 2011.

Wersin, P., E. Curti, C.A.J. Appelo, Modelling bentonite-water interactions at high solid/liquid ratios: swelling and diffuse double layer effects. Appl. Clay Sci. 26: 249-257, 2004.

Zuidema, P., Advancements in Deep Geological Disposal of Radioactive Waste through International Cooperation: The Role of Underground Laboratories – Mont Terri Project, Proceedings of the 10 Year Anniversary Workshop, pp 69-71, Rep. Swiss Geol. Surv. 2, 2007.